Expression of *Arabidopsis thaliana* Cellulose Synthase Proteins and Associated Proteins in a *Spodoptera frugiperda* cell line

By

Jessy Lyons

A thesis submitted to The Faculty of Science (Applied Bioscience Program)

in conformity with the requirements

for the degree of Master of Science

University of Ontario Institute of Technology

Oshawa, Ontario, Canada, 2012

Abstract

Understanding how cellulose synthesis occurs is key to understanding the formation of the plant cell wall. This understanding could also be key to modifying cellulose production to permit more efficient extraction of glucose from cellulose for the production of biobased materials. Cellulose biosynthesis is carried out by cellulose synthases; transmembrane multimeric processive glycosyltransferases responsible for polymerizing UDP-glucose into glucan chains. Thirty-six glucan chains bind together in parallel to form elementary cellulose microfibrils. Due to the essential nature of cellulose synthases for plant survival and the recalcitrant nature of the cell wall to chemical and enzymatic digestion, the cellulose synthases can be very difficult to analyze by traditional approaches. In an attempt to circumvent some of the issues of studying cellulose synthases, the cellulose synthase genes *CESA1* and *CESA3*, along with the cell wall associated genes *COBRA, DET3 and POM1* were recombined into an engineered *Autographa californica nucleopolyhedron virus* and expressed in *Spodoptera fruigiperda* ovarian cells. Although recombinant protein could be detected for CESA1 and CESA3, C^{14}-glucose incorporation on baculovirus infected cell lines have given inconclusive results to the cellulose synthase activity of the CESA1 and CESA3 proteins. With further optimization of the protein expression of CESA1 and optimization of the variability in the C^{14}-glucose incorporation assays, the baculovirus system may prove a useful tool for studying the cellulose synthases.

Acknowledgments

I would like to offer my gratitude to my supervisor, Dr. Dario Bonetta, who has given me this opportunity to do this masters and was there to give advice and encouragement when it was needed. He allowed me to make mistakes, learn and develop my critical thinking and troubleshooting skills.

I would also like to thank the members of my committee, Dr. Ayush Kumar and Dr. Janice Strap for their expertise, support and advice to guide me in the right direction.

I would like to thank my colleagues from the Applied Bioscience Program at the University Of Ontario Institute Of Technology for their help and perspective.

Finally, I would like to thank my Fiancée Jessica and my family for their constant support during my studies.

Table of Contents

List of Figures

List of Tables

List Abbreviations

ACMNPV	*Autographa californica* multicapside nucleopolyhedronvirus
ATP	Adenosine Tri-Phosphate
BCA	Bicinchonic Acid
BiFC	Bimolecule Fluoroescent Complementation
BR	Brassinosteroids
BSA	Bovine Serum Albumin
CaZY	Carbohydrate Active Enzyme Database
cDNA	complementary Deoxyribonucleic Acid
CDS	Protein Coding Sequence
CESA	Cellulose Synthase A
CFP	Cyan Fluoroescent Protein
CoIP	Co-Immunoprecipitation
CoRE	Conditional Root Expansion
CPM	Counts Per Minute
CSC	Cellulose Synthase Complex
CTL	Chitinase Like
dGTP	Deoxyguanosine Triphosphate
DMSO	Dimethyl sulfoxide
E. coli	*Escherichia coli*
ECL	Enhanced Chemiluminescence
FITC	Fluorescein isothiocyanate

GT	Glycosyl Transferase
HSV1-TK	Herpes Simplex Virus - Thymidine Kinase gene
kDa	Kilodalton
LB	Luria-Bertani
MAP	Microtubule Associated Proteins
MOI	Multiplicity of Infection
MYC	Myelocytomatosis
PBS	Phosphate Buffered Saline
PBST	Phosphate Buffered Saline Tween 20
PCR	Polymerase Chain Reaction
PE	Phycoerythrin
pfu	Plaque Forming Units
psi	Pounds Per Square Inch
RIPA	Radio Immuno Precipitation Assay Buffer
SDS	Sodium Dodecyl Sulphate
SDS-PAGE	Sodium Dodecyl Sulphate - Polyacrylamide Gel Electrophoresis
SF9	*Spodoptera frugiperda*
TAIR	The Arabidopsis Information Resource
Topo	Topoisomerase
UDP	Uridine Diphosphate
YFP	Yellow Fluoroescent Protein

Introduction

Cellulose

Cellulose is the most abundant polymer in plant cell walls, comprising approximately one third of plant biomass, and is the main structural polymer of plants (Somerville, 2006). The repeat unit of cellulose is glucose, linked together by β-1,4-glycosidic linkages from its activated form UDP-glucose. Each of these repeating subunits of glucose will bind 180^{o} inverted to the previous subunit to form cellobiose. These repeating units will extend 500-14000 glucose molecules long, with 36 polymer chains hydrogen bonding together, parallel to one another, to form single cellulose microfibrils (Somerville, 2006). These strands are highly ordered and have a crystalline nature making them strong enough to resist the internal turgor pressure of plant cells and create a support structure for the plant. This crystalline nature of cellulose makes it difficult to hydrolyze both through enzymatic and chemical methods (X. Li, Weng, & Chapple, 2008). Cellulose is also surrounded by a number of other polymers in the cell wall including lignin, pectin and hemicelluloses which further stabilize the cell wall and inhibit the extraction of glucose through enzymatic hydrolysis (Cosgrove, 2005). Cellulose can occur in two forms, cellulose I and cellulose II. Cellulose I is the naturally occurring form and is characterized by the parallel alignment of the glucan chains. Cellulose II which is not naturally occurring contains glucan chains which are anti-parallel to one another (Somerville, 2006). Cellulose II is formed when cellulose I is exposed to a highly alkali environment, a process known as mercerization. Cellulose II is more stable than cellulose I due to increased hydrogen bonding between the glucan chains (Simon, Glasser, & Scheraga, 1988) .

Cellulose is of great interest to both governments and corporations in an attempt to offset the reliance on fossil fuels and increase the efficiency of the production of biofuels, textiles and cattle feed (X. Li, et al., 2008). With cellulose being the most abundant polymer in the environment and its simplest unit being glucose, it is possible for cellulose to be an abundant source of energy for fermentation into

bioethanol fuel or the direct consumption by livestock (X. Li, et al., 2008). Due to cellulose's crystalline nature and resistance to hydrolysis, this abundant source of glucose is not economically accessible. By modifying the cellulose or cell wall composition of current food crops it may be possible to harvest the cellulose from the unused portions of the food crops and increase the useful yield of each crop. It may also be possible to avoid food crops and rich farm land altogether by bioengineering the cellulose availibility of C4 grasses such as *Miscanthus giganteus,* which can tolerate growing conditions that are not beneficial for food crops, and optimize the availability of the plants cellulosic glucose. Currently two approaches to improving the accessibility of glucose are underway. The first is the pre-treatment of the cell wall to remove unwanted polymers via exposure to lignocellulases and ligninases, followed by the enzymatic hydrolysis of cellulose. This approach could become very expensive due to the cost of manufacturing industrial quantities of enzymes. The second approach is genetic engineering of potential biofuel crops to increase glucose availability, increase cellulose biomass, incorporate ligninase genes into potential biofuel crops and to reduce the crystallinity of cellulose (Sticklen, 2006). In order to engineer biofuel crops to increase the cellulose biomass or increase glucose availability, it is vital that the enzymes responsible for the synthesis and regulation of cellulose be well understood.

Glycosyltransferases

Glycoslytransferases (GTs) are ubiquitous enzymes that can be found in plant, mammalian and bacterial species. GTs are enzymes that catalyze the linkage of a sugar nucleotide to a saccharide or non-saccharide acceptor. Sugars, proteins, lipids and nucleic acids can all be glycosylated by GTs. These classes of proteins are all involved in the synthesis of sugar based polymers. There are two major types of GTs, processive and non-processive (Farrokhi et al., 2006). Processive glycosyltransferases are involved in polysaccharide synthesis and will repeatedly attach sugar molecules to the previous sugar creating long polysaccharide polymers. Processive glycosyltransferases have also

been shown to work in tandem, in the case of hyaluronan synthase; two glycosyltransferases alternate in the addition of N-acetyl-glucosamine and glucaronic acid to form the hyaluronan polymer (Coutinho, Deleury, Davies, & Henrissat, 2003). Non-processive glycosyltransferases will attach a single sugar molecule to an acceptor molecule to form a glycosylated molecule, such as glycolipids and glycoproteins. Each glycosyltransferase enzyme will glycosylate a specific donor substrate to a specific acceptor molecule, with the large variation in donor molecules and almost unlimited number of acceptor molecules there is the possibility of an exceptional number of different GTs (Coutinho, et al., 2003). To classify the different GTs, a Carbohydrate-Active EnZyme database was created (Cantarel et al., 2009). The database sorts GTs based on type of protein folding motif, whether they invert or maintain the substrate stereochemistry and what type of substrates and acceptors they catalyze (Coutinho, et al., 2003). Classifying by form and function rather than sequence homology helps make associating proteins simpler when compared to classifying by domain. Domain classification can make determination of GTs confusing, for example many of the processive GTs contains a DxD motif in the catalytic site. The swissprot database shows 51% of all proteins in the database containing a DxD motif (Coutinho, et al., 2003). The presence of a DxD motif in a protein could be misleading in classification. There are currently 94 families of GTs in the database (http://www.cazy.org/GlycosylTransferases.html, June 19 2012). Approximately 1.6% of the *Arabidopsis* genome encodes for more than 400 genes that have been identified as GTs (Farrokhi, et al., 2006). Of the over 400 glycosyltransferase genes in *Arabidopsis*, only 9 have been directly linked to the production of cellulose.

Cellulose Synthases (CESA)

Cellulose Synthases are members of the GT2 family of β-glycoslytransferases and a sub-member of the family of endo-1,4-glucanases (Saxena, Brown, & Dandekar, 2001). Other enzymes similar to cellulose synthase in this group are hyaluronan synthase and chitin synthase **(Table 1).** A defining motif across the β-glycoslytransferases is a

conserved D, D, D, Q/RXXRW protein sequence. This motif is thought to be an active component in the catalytic site for the polymerization of glucans (Saxena, et al., 2001). Cellulose synthases also contains several other important domains thought to be important for their function. For example, the N-terminus contains a zinc finger domain, with a highly conserved repeating CXXC motif. This domain is believed to be involved in protein-protein interactions (Richmond, 2000). The CESAs also contains eight transmembrane domains which are thought to create a pore for passing glucan chains from the cytosolic side to the extracellular side of the plasma membrane. Two of the transmembrane regions occur N-terminally to the catalytic domain and the remaining six transmembrane domains occur C-terminally to the catalytic domain (**Fig. 1** (Richmond, 2000)).

The Cellulose Synthase Complex (CSC) is the core component required for synthesis of cellulose microfibrils. *Arabidopsis thaliana* contains a total of 10 cellulose synthase genes. *CESA1* (At4G32410), *CESA2* (At4G39350), *CESA3* (At5G05170), *CESA5* (At5G09870), *CESA6* (At5G64740) and *CESA*9 (At2G21770) are responsible for the synthesis of the primary cell wall, with CESA1 and CESA3 always required, whereas CESA2, CESA5 and CESA6 are expressed in a tissue dependent manner. *CESA4* (At5G44030), *CESA7* (At5G17420) and *CESA8* (At4G18780) are responsible for the synthesis of the secondary cell wall. CESA10 has shown mRNA expression but has no known function to date and has not been shown to be directly involved the CSC (Liepman, Wightman, Geshi, Turner, & Scheller, 2010; Persson et al., 2007). The protein CSI1 has been implicated in linking the CSC to the microtubules (S. Li, Lei, Somerville, & Gu, 2012).

An elementary cellulose microfibril is thought to consist of 36 glucan chains. The formation of the microfibril is thought to be accomplished by the formation of a cellulose synthase “rosette” or terminal complex. The rosette is a hexameric cellulose producing enzyme complex (**Fig. 2)**. Six glucan chains are formed from each of the six complexes (Kimura et al., 1999). Knockdown of *CESA1* and *CESA3* RNA transcripts have

shown that the elimination of either these genes results in a lethal phenotype; cellulose synthesis is too severely impaired for survival (Somerville, 2006). In addition the *rsw1* mutation, a mutation that reduces the protein stability of *CESA1*, shows a radial swelling phenotype when grown at a restrictive temperature of 31^{o}C. The radial swelling phenotype is linked to a reduction in cellulose production. The *rsw1* mutation appears to cause instability in the rosette preventing it from properly forming at a temperature above 31^{o}C, therefore preventing the synthesis of cellulose. Wildtype cellulose production is recovered when the plants with rsw1 are grown at permissive temperature of 18^{o}C (Arioli et al., 1998). These two studies have shown that CESA1 and CESA3 are both necessary in the CSC. CESA1 and CESA3 are also functionally different to one another and are not interchangeable. CESA3 overexpression in an *rsw1* mutant does not compliment the *rsw1* mutation and the mutant phenotype persists (Burn, Hocart, Birch, Cork, & Williamson, 2002). Coimmunoprecipitation studies of the CSCs have shown direct interaction of CESA3 and CESA6 (Desprez et al., 2007). This was confirmed by bimolecular fluorescent complementation (BiFC) tagging of CESA3 and CESA6 proteins (Amor, Haigler, Johnson, Wainscott, & Delmer, 1995). These studies have shown that these CSCs are composed of at least three of the cellulose synthase paralogs, with CESA1 and CESA3 always present and CESA6 associating with CESA3 (Desprez, et al., 2007). The study of the expression patterns of *CESA6, CESA2* and *CESA5* in different tissues and the use of double and triple *CESA* mutant knockout studies have alluded to the partial redundancy of the CESA2, 5 and 6 (Desprez, et al., 2007). The when two of the three gene expressions of CESA2, 5 and 6 are knocked down the third gene can compensate, allowing for a dwarfed but non-lethal phenotype (Desprez, et al., 2007). Peredez (2006), has provided evidence that CSCs move along microtubules. Co-localization between the CSC and the microtubules was observed with yellow fluorescent protein (YFP) tagging of CESA6 and cyan fluorescent protein (CFP) tagging of the TUA1 microtubule protein and was visualized by spinning disk confocal microscopy (Paredez, Somerville, & Ehrhardt, 2006). The spinning disk confocal microscopy allowed for high resolution 3D images to be taken of the plant cells and capture the movement

of the fluorescent tags. This suggests that the organization of cellulose microfibrils is guided by the cortical microtubules. The cortical microtubules are controlled by the Microtubule-Associated Proteins (MAP) such as the protein MOR1 (Sugimoto, Himmelspach, Williamson, & Wasteneys, 2003). A mutation of the MOR1 causes cortical microtubule organization to become inhibited when plants are incubated at restrictive temperature of 28^{o}C or above. Long exposure to temperatures above 28^{o}C cause morphological defects including twisting of organs, isotropic cell expansion and impared root hair polarity (Whittington et al., 2001). It is possible that cellulose microfibril organization is controlled indirectly by the regulation of the plant cortical microtubules.

Cellulose Synthase Associated Proteins

There have been a number of non-cellulose synthase proteins discovered that have an impact on the deposition of cellulose in plants. Many of these proteins are indirect interactions as they are not found during CESA Co-Immunoprecipitation (CoIP) experiments, but are shown to have an effect on cellulose synthesis when their activity is inhibited (Desprez, et al., 2007). These indirect interactions may have many associated functions. They may orient the path of the CSC, help in assembly and movement of the CSC to the membrane, link the cellulose to the other cell wall polymers or have cellulase activity to cut the existing cellulose which will allow the cell to expand and new cellulose to be deposited.

A group of mutations that have an indirect impact on cellulose deposition are known as the Conditional Root Expansion mutants (CoRE). Wild type root cells exhibit an anisotropic shape where the longitudinal length is much greater than the radial diameter of the cells (Hauser, Morikami, & Benfey, 1995). CoRE mutations result in dramatically reduced cell elongation with a variation in radial diameter. Hauser et al. (1995), characterized 21 mutations at six loci that have CoRE phenotypes. These mutations can be separated into two groups based on radial expansion. Mutant's *cob1*,

qui1, and *cud1* show a greater diameter than longitudinal length suggesting that polarity of expansion has been changed to be perpendicular to the root. The mutants *lit1*, *pom1-1* and *pom2-1* showed loss of the anisotropic shape and became spherical (Hauser, et al., 1995). CoRE mutant phenotypes are conditional upon the roots growing at maximum rate. These high rates of root growth are achieved through the use of a high sucrose concentration, 4.5% sucrose, nutrient agar as a media for the *Arabidopsis* seedlings (Hauser, et al., 1995). The high sucrose agar is readily employed as a carbon source by the plants, allowing them to grow very rapidly. To rule out osmotic effects caused by the high sucrose content, mannitol was substituted for sucrose as mannitol is not a carbon source for *Arabidopsis*. The mannitol agar showed no phenotypes in wildtype or the mutant strains, ruling out osmotic effect as the cause of the CoRE phenotype (Hauser, et al., 1995).

It has been proposed that the COBRA (COB1, At5G60920) protein is related to the ability of *Arabidopsis* to elongate cells into an anisotropic shape during rapid cell expansion rather than expand into a spherical shape. COBRA has been determined to contain a glycophosphatidylinsositol-anchored (GPI) domain and a domain of unknown function. COBRA is localized extracellularly to the longitudinal sides of the plasma membrane (Roudier et al., 2005; Schindelman et al., 2001). It was initially believed that COB aligned the microtubules within the plant cell to regulate cellulose microfibril deposition, but the *mor1-1* mutation has shown otherwise. The *mor1-1* mutation disrupts cortical microtubules at 29^{o}C. These *mor1-1* mutants lose the ability to achieve anisotropic cell expansion but the cellulose microfibril deposition maintained a transverse microfibril orientation (Sugimoto, et al., 2003; Whittington, et al., 2001). Instead it appears that the cortical microtubules are directly or indirectly required to localize the COB protein along the plasma membrane. When cortical microtubules were inhibited by the *mor1-1* mutation there was a reduction in the localization of COB to the membrane, indicating that COB is associated to the microtubules (Roudier, et al., 2005). The mechanism of COBRA is still to be determined but it seems likely to regulate cell

cellulose deposition in the cell wall as it relates to cell expansion (Schindelman, et al., 2001).

Another CoRE protein that shows association with cellulose microfibrils is POM1-1. The mutant *pom1-1* phenotype shows a loss of anisotropic elongation and an increase in the total volume of the cell over the volume of wild-type, in all directions (Hauser, et al., 1995). The mutant phenotype also includes ethylene overproduction, reduced tolerance of abiotic stress and ectopic deposition of lignin (Sanchez-Rodriguez et al., 2012). POM1 is also referred to as CTL1 for its chitinase-like domain, which does not have chitinase activity (Hermans, Porco, Verbruggen, & Bush, 2010). Cell biology experiments have shown that the *pom1-1* mutation reduces the velocity of CSC across the plasma membrane by approximately 40% resulting in a reduction of cellulose deposition (Sanchez-Rodriguez, et al., 2012). By exposing purified MYC fused POM1-1 protein to the insoluble wall fractions of etiolated seedlings, commercial xyloglucan and fibrous cellulose, then immunoblotting with an anti-MYC antibody, it was found that POM1-1 preferentially bound to glucan chains (Sanchez-Rodriguez, et al., 2012). With the interaction of POM1-1 with both the CSCs and glucan chains it is hypothesized that POM1-1 is involved in crosslinking cellulose and hemicelluloses (Sanchez-Rodriguez, et al., 2012).

The protein DET3 has been mapped to subunit C of a vacuolar ATPase in *Arabidopsis thaliana*. V-ATPases primarily function in the *Arabidopsis* active transport system as proton pumps to adjust the pH gradient between the external and internal environment and they also have been implicated in metabolite homeostasis (Dettmer, Hong-Hermesdorf, Stierhof, & Schumacher, 2006). The *det3* mutant is dwarfed in both dark and light conditions due to reduced cell elongation and has a highly reduced response to brassinosteroids (BR). In wild-type *Arabidopsis,* the addition of BRs will stimulate an increase in hypocotyl length, *det3* mutants show no increase in hypocotyl length with addition of BRs showing an inhibition of the BR response (Schumacher et al., 1999). It has been determined that V-ATPases in plants are also responsible for

endocytic and secretory trafficking (Dettmer, et al., 2006). DET3 has also been implicated in the transfer of signalling oxylipins, ethylene and jasmonic acid (Brux et al., 2008). It seems likely this trafficking is also responsible for the reduced response to BRs. Interestingly, *det3* mutants also show a cellulose deficiency and a hypersensitivity to isoxaben, which possibly links the *det3* to destabilization of the cell wall. It is possible that DET3 is responsible for trafficking cellulose biosynthesis proteins to the cell membrane or that the defect lies in the inhibition of cellulose biosynthesis proteins that are located in the Golgi (Brux, et al., 2008).

Expression of cellulose biosynthesis related proteins in non-plant host

Due to the resilient nature of the plant cell wall and its integral role in the survival of the plant, many experiments become difficult or impossible to achieve. The determination of gene function is often done using loss of function mutations or gene function knock out experiments. If genes that are vital to the survival of the organism are inhibited, the organism to be studied will not survive. As an example, CESA1 cannot be completely inhibited without causing lethal phenotype to the plant (Somerville, 2006). Therefore within the plant system it is impossible to determine if CESA3 and CESA6 alone will have any cellulose production due to the requirement of CESA1 for the organism's survival. Similarly, due to the strength and insolubility of the cell wall it is highly difficult to remove the cell wall to take high resolution images of the membrane, probe with antibodies and more difficult to remove the cell wall without killing the cell itself. By expressing cellulose synthase genes in a non-plant system it may be possible to further study these proteins that cannot easily be studied within the plant itself. Since these added genes are not necessary to the survival of the host organism there modification or lack of function will not result in a lethal phenotype. To accomplish this non-native expression, plant genes will be infected into the insect cell line *Spodoptera frugiperda* (SF9) and analyzed for expression and activity. SF9 cells are easily cultured and maintained without the requirement of specialized equipment making them cost-effective and easy to use. SF9 cells are also easily infected by the *Autographa californica*

multiple nucleocapsid polyhedron virus (AcMNPV). This virus has been modified to be recombined with any gene of interest allowing for rapid high yield expression of the protein of interest within the SF9 cell line (Dee & Shuler, 1997). SF9 via AcMNPV expression of the 8 transmembrane domain protein Menkes copper transporting P-type ATPase has shown high yield and protein catalytic activity (Hung, Layton, Voskoboinik, Mercer, & Camakaris, 2007). This protein has structural similarities to the cellulose synthases and makes the SF9 expression system a promising candidate for the expression of cellulose synthases.

Hypothesis

By expressing *Arabidopsis thaliana* cellulose synthase genes within a *Spodoptera frugiperda* ovarian cell line, which contains similar mechanisms of glycosylation to *Arabidopsis* and has the ability to express native processive glycosyltransferases, it should be possible to synthesize active *Arabidopsis* cellulose synthase proteins and determine the minimum number of protein constituents required to achieve cellulose synthesis.

Thesis Objectives

i) To design and engineer *Autographa californica* multiple nucleopolyhedronvirus constructs containing the protein coding sequence of the genes *CESA1, CESA3, COBRA, POM1* and *DET3.* Each cloned gene will also contain a designed N-terminal fusion sequence of an antibody epitope tag for protein detection.

ii) To analyze the expression of the target protein for each viral construct by determining the level of protein expression and if the protein is localizing to the membrane fraction of the SF9 cells.

iii) To determine the status of the cellulose synthesis activity for each of the proteins and to determine if combinations of the expressed proteins will lead to an effect on the level of cellulose activity.

Materials and Methods

Amplification of target genes

All *Arabidopsis* genes used in the experiments were from the Columbia (Col-0) ecotype. *CESA1* and *CESA3* were amplified from cDNAs donated by Robert Law. The genes *COBRA, POM1* and *DET3* were amplified from full length cDNA clones acquired from the *Arabidopsis* Biological Resource Center at Ohio State University (Yamada et al., 2003). In an attempt to distinguish each gene product, different epitope tags were designed for each overexpression construct **(Table 2).** Genes were amplified using Phusion High Fidelity DNA polymerase (NEB; Ispwich, MA). The manufacturer's recommended reaction mix and PCR conditions were followed for the use of the Phusion polymerase. Amplified products were gel purified using the BioBasic gel extraction kit (Biobasic; Markham, ON).

Primer Design

Primers were designed for each gene to incorporate the full length cDNA sequence, add a unique N-terminal fusion epitope tag to the CESAs, a C-Terminal fusion tag to the associated proteins and a CACC topoisomerase (Topo) recognition sequence to the 5` end of the primary strand for cloning into the pENTR/D-topo plasmid (Invitrogen; Carlsbad, CA) **(Table 3)**.

Touchdown PCR Amplification

For difficult amplicons that resulted in large amounts of nonspecific products a touchdown PCR protocol was employed. In a touchdown PCR the initial annealing temperature is set to 4^{o}C above the melting temperature of the primer set. For the first 8 cycles the annealing temperature is reduced 1^{o}C per cycle. After the 8 cycles, the PCR is continued another 30 cycles at the lowest annealing temperature at the end of the

end of the 8 cycles. By slowly lowering the annealing temperature over the first 8 cycles it ensures that the most stable primer binding becomes the dominant fraction of PCR products. The reaction mixes were completed as per the polymerase manufacturer specifications. The PCR conditions for a touchdown reaction are shown in **(Table 4)**.

Cloning of target genes

Amplified products were ligated into the pENTR/D-topo plasmid **(Figure 3.)** using the 5' CACC topoisomerase recognition sequence to insert the fragment directionally. Cloning reaction conditions were completed according to the manufacturer's specifications. Cloning reactions were transformed into chemically competent DH5α *E. coli* via heat shock according to Sambrook & Russell (2001). Plasmid preparation from *E. coli* was accomplished via alkaline lysis followed by phenol/chloroform extraction as recommended in Sambrook & Russell (2001).

Confirmation of Plasmid Constructs

Plasmid constructs were subjected to double restriction digests to confirm the presence and directionality of the insert. By choosing restriction enzymes that would cut within the insert and within the plasmid, it could be determined what the total size of the construct was and based on the calculated fragmentation size what the directionality of the insert was. The plasmids were then completely sequenced via Sanger sequencing on a capillary based ABI3730XL at The Centre for Applied Genomics in the Hospital for Sick Children. The inserts were sequenced along their entire length using primers flanking the insert from within the vector and nested primers from within the insert sequence **(Table 5)**.

Restriction Digest

Restriction digests were performed using restriction enzymes acquired from New England Biolabs (Ipswich, MA). The enzyme cut sites were determined using the CLC genomics workbench (CLC bio, Denmark). The restriction digests were performed in 10 µl volumes; using 1 µl of manufacturer suggested 10x buffer, 0.5 µl of the required enzyme. The desired amount of DNA was added and the volume made up to 10 µl with water. The reactions were digested at 37^{o}C for 1 h. Double digests were performed in the same manner but with the addition of a second enzyme.

Sequence Alignments

The sequencing reads of each gene cloned into pENTR/D-topo were aligned to their respective cDNA sequences acquired from The Arabidopsis Information Resource (TAIR) database. The sequencing reads were aligned to the reference sequences using the CLC Genome Workbench 3.6.5 (CLC Bio, Denmark) sequence alignment tools. Any basepair alignment conflicts flagged by the software were examined visually and determined to be either an incorrect alignment by the software or an actual base pair variation within the sequence. If the alignments showed no sequence variations that would alter the expressed protein, the gene inserts were considered to be without error.

Plasmid Maps

Annotated plasmid maps were downloaded from GenBank (Benson, Karsch-Mizrachi, Lipman, Ostell, & Wheeler, 2005) and imported into CLC Genome Workbench 3.6.5 (CLC Bio, Denmark). Any plasmid sequences not annotated in Genbank were manually annotated **(Figure 6)**.

Cultivation and growth conditions for bacteria

Luria-Bertani (LB) medium was used to cultivate DH5α *E.coli* for transformation and selection. LB media was made at 2 fold concentration (20 g tryptone, 10 g yeast extract, 20 g NaCl , 1 L of H_2O) and autoclaved at 121^oC. The media was diluted 1:1 with sterile water for use in liquid culture. For agar plates, the 2 x LB media was diluted 1:1 with 2 x Agar (30 g agar, 1 L of H_2O). Any required antibiotics were added immediately prior to use.

Gene recombination into *Autographa californica* Multiple Nucleocapsid Polyhedron Virus (AcMNPV)

The Gateway expression system, developed by Invitrogen, enables site specific recombination from entry vector such as pENTR/D-topo into a destination vector. Currently, Invitrogen has a variety of destination vectors for expression in mammalian, bacterial, insect and yeast hosts. The site specific recombination is dependent on the attL1 and attL2 viral recombination sites. These recombination sites maintain the reading frame of the sequence and match it to the reading frame of the destination vector. Because the recombined insert is in frame with the destination vector, the gene product can be fused N-terminally or C-terminally to additional sequences upstream or downstream of the recombination site such as epitope tags or fluorescent proteins. Since the goal was to express the chosen genes in an insect cell line the Baculodirect N-terminal expression kit was chosen. The Baculodirect N-terminal expression kit (Invitrogen; Carlsbad, CA) contains a V5 N-terminal fusion tag which allows for V5 antibody binding to the expressed protein and a polyhedron promoter up stream of the recombined gene providing a high level of gene expression.

Recombination of pENTR/D-topo constructs with the ACMNPV baculovirus was done according to the manufacturer's specifications (10 µl of supplied baculovirus DNA, 300 ng of pENTR/D-topo plasmid, 4 µl TE buffer pH 8.0, 4 µl of LR Clonase II enzyme mix. Incubate samples at 25^oC for 18 hours). The recombined viral DNA was then transfected

into *Spodoptera frugiperda* (SF9) cell line using the cationic lipid reagent, Cellfectin II, according to the Invitrogen manual. Once the viral DNA was transfected into the SF9 host, the virus was able to self-replicate. Amplification of non-recombinant viruses was inhibited by the Herpes Simplex Virus – Thymidine Kinase gene (HSV1-TK) located at the recombination site of the non-recombined virus. The HSV1-TK gene functions in conjunction with the chemical ganciclovir. Ganciclovir **(Figure 4)** is a synthetic analogue of deoxyguanosine triphosphate (dGTP) and competitively inhibits the incorporation of dGTP. The incorporation of ganciclovir into the viral DNA strand results in the termination of DNA elongation. This allows only recombined viral DNA, which has lost the HSV1-TK gene, to replicate. The viral stock produced after transfection is referred to as the P0 stock.

Spodoptera frugiperda (SF9) growth conditions

The SF9 cells used in these experiments were acquired from Gibco in 1.5 ml of frozen media with 7.5% DMSO, which contained approximately $1.5x10^7$ cells. The SF9 cells were adapted by Gibco to serum free media. SF9 cells were grown as adherent culture in 75ml T-flask containing 12ml of SFM900-II media from Gibco and supplemented with 10ug/ml gentamycin to prevent contamination. Cells were housed in a 28^oC incubator and passaged every 4-5 days when cell confluency reached 90%. Passaged cells were seeded at a dilution of 1:5.

SF9 Cell Counting

A bright Line Counting Chamber (Hausser Scientific; Horsham, PA) was used to count the SF9 cells. The chamber employs the Improved Neubauer ruling pattern. Fifty µl of SF9 cells in media was combined with 50 µl of Trypan blue. Trypan blue is a vital stain that stains dead tissue blue, this allows the ratio of living cells to dead cells to be determined. 10 µl of the mixture was loaded into the counting cell. The cell was viewed

on a Leica DM IL LED (Leica Microsystems Inc.; Concord, ON) inverted microscope at 100x magnification. The cells were counted in a region of 1 mm^2 = 0.00625 µl volume and from that the number of cells/ml was calculated.

Recombinant baculovirus enrichment

To increase viral titres and select against non-recombinant viruses, 20 µl of P1 viral stock was added to a 75ml T-flask containing SF9 adherent cells in log phase growth with 12 ml of SFM900-II media, 10 µg/ml gentamycin and 100 µM ganciclovir. After 96 hours the media was collected to harvest the budded baculovirus. The new collected viral stock became the P1 stock. The process was repeated until a P4 stock was collected.

Viral titer of Baculoviruses

Titering of baculovirus stocks was accomplished through the detection of the cell surface protein, gp64. This protein is an *Autographa californica nucleopolyhedronvirus* (AcMNPV) specific protein which is expressed during early infection stages. Serial dilutions of each virus were done at 1:10, 1:100, 1:1000, 1:10000 in SFM900-II media. A baculovirus standard of known plaque forming units per ml (pfu/ml) was serially diluted to the same dilutions as the samples to establish a standard curve of pfu/ml. 100 µl of SF9 cells at a concentration of $2x10^6$ cells/ml was dispensed into 1.5 ml microtubes. 100 µl of each viral dilution was added to its own tube of SF9 cells. SF9 cells without baculovirus were used as a negative control. All cells were incubated for 18 hours at 28^oC in an orbital shaker. After 18 hours the cells were centrifuged at 1800 rpm for 3 minutes in an Eppendorf 5424 centrifuge. Media was aspirated off the cells and 50 µl of gp64-PE antibody (Expression Systems; Woodland, CA) diluted 1:500 in 1X PBS was added to the cells. Cells were then incubated with the antibody for 20 minutes at 4^oC. 150 µl of cold PBS was added to each tube and the cells were again centrifuged for 3 minutes at 1800 rpm. Supernatant was aspirated and the cells were washed with 200 µl

of cold PBS and centrifuged. The PBS wash step was repeated 3 times. The cells were resuspended in 200 µl of PBS. The cells were analyzed on a Guava PCA flow cytometer, which allows for simultaneous cell counting and detection of the gp64-PE antibody (Millipore; Billerica, MA). The ratio of cells expressing gp64 to cells not expressing gp64 allows the viral titre to be determined when compared to the standard viral dilutions.

Whole Cell Protein Extraction

Infected SF9 cells collected from their flask or plate and transferred to an appropriately sized tube, typically a 15 ml conical tube or 2 ml microtube. The cells were centrifuged at 3000 x *g* and the supernatant was aspirated. The cells were then solubilized in Radio Immuno Precipitation Assay (RIPA) buffer (150 mM NaCl, 0.1% Triton X-100, 0.5% sodium deoxycholate, 0.1% sodium dodecyl sulphate (SDS), 50 mM Tris-HCl pH 8.0 and a general use protease inhibitor cocktail P2714 (Sigma Aldrich)). For a single T-75 flask of SF9 cells 300 µl of RIPA buffer was added, for a single well (9.6 cm^2) in a 6-well plate, 50 µl of RIPA buffer was used to solubilize the SF9 cells. Cells and buffer were vortexed and the samples were stored at -20^oC.

Membrane Protein Extraction

Infected SF9 cells were collected from their flask or plate and transferred to a 15 ml conical tube. The cells were centrifuged at 3000 x *g* and the supernatant was aspirated. 10 ml of membrane extraction buffer was added (50 mM HEPES pH 7, 10 mM $MgCl_2$, 0.4 M sucrose). The samples were lysed by passage through a French Pressure Cell (Thermo Fisher Scientific) at an internal pressure of 30,000 psi. The samples were transferred to 10 ml ultracentrifuge tubes and centrifuged at 105,000 x *g* for 1 hour at 4^oC in a Sorvall Discovery 90SE ultracentrifuge (Thermo Fisher Scientific). The samples were decanted and resuspended in membrane solubilisation buffer. Membrane solubilisation buffer contains 50 mM HEPES, 150 mM NaCl, 10% v/v glycerol, 2 mM 2-

mercaptoethanol, 3 mM Triton X-100 and a general use protease inhibitor cocktail P2714 (Sigma Aldrich)). For a T-75 flask sample the pellet was dissolved in 200 µl of membrane solubilisation buffer; for a single well of a 6-well plate 50 µl of membrane solubilisation buffer was used. The samples were vortexed and stored at -20^{o}C.

BCA Protein Assay

Protein concentration was measured using a bicinchonic acid (BCA) protein assay kit (Pierce; Rockford, IL). The BCA assay was performed slightly modified from the manufacturer's instructions. In short, 75 µl of diluted sample was added to 75 µl of BCA dye in a 96 well plate format (Sarsdedt; Nümbrecht, Germany). The plate was incubated for 2 h at 37^{o}C. The absorbance of the plate was read at 562 nm and corrected against a solution containing buffer and BCA dye. The corrected absorbances were compared to a BSA standard curve to determine the protein concentrations of the samples.

Sodium Dodecyl Sulfate Polyacrylamide Gel Electrophoresis (SDS-PAGE)

Protein separation from recombinant cell lines was achieved by SDS-PAGE using a BioRad mini-protean III system. Typically, 40 µg of protein was loaded per well when a 10 well comb was used. Protein samples consisted of 5 parts protein extract and 1 part 5x loading buffer (LD; 10% w/v SDS, 10 mM 2-mercaptoethanol, 20% v/v glycerol, 0.2 M Tris-HCl pH 6.8, 0.05% w/v Bromophenol blue). The samples were vortexed briefly and incubated at 70^{o}C for 10 minutes. The samples were returned to ice after the heating and loaded into the SDS-PAGE gel. The SDS-PAGE gels consisted of a 5% stacking layer and a 10% resolving layer according to (Sambrook & Russell, 2001). A broad range molecular weight standard (Bio-Rad, Mississauga, ON) was run in the first lane of each gel. The gels were electrophoresed at a constant 130V for approximately 1 hour in running buffer (25 mM Tris-HCl, 190 mM glycine, 0.1% SDS). The gels blotted onto nitrocellulose paper.

Western Blotting

Semi-Dry Protein Trans-blotting

Protein was transferred from SDS-PAGE gels onto nitrocellulose paper using a Trans-Blot Semi-Dry Transfer Cell (Bio-Rad, Mississauga, ON). The nitrocellulose paper and two pieces of extra thick filter paper were equilibrated in Towbin transfer buffer (25 mM Tris, 192 mM glycine, 20% methanol, pH 8.3) for 30 minutes prior to transfer. The SDS-PAGE gel was equilibrated in Towbin transfer buffer for 10 minutes prior to transfer. The transfer components are assembled from bottom to top; filter paper, nitrocellulose paper, SDS-PAGE gel, filter paper. The transfer sandwich was rolled with a serological pipette to remove any air bubbles that would interfere with the transfer. On the Trans-Blot system, SDS-PAGE mini gels were run at 5.5 mA/cm^2. Typically gels were run at 80 mA constant current for 1 hour to ensure transfer of the large proteins of interest to the nitrocellulose.

Ponceau S Staining

The nitrocellulose blot was temporarily stained with Ponceau S solution (0.1% w/v Ponceau S, 5% acetic acid in dH_2O) after semi-dry transblotting to confirm successful protein transfer from the SDS-PAGE gel onto the nitrocellulose blot. The nitrocellulose blot was incubated in the Ponceau S solution on a bidirectional rotator for 10 minutes and then rinsed with repeated water washes until the background was removed and the protein bands were visible. The nitrocellulose blot was incubated in Phosphate Buffered Saline + Tween 20 (PBST; 14 mM NaCl, 1.5 mM KH_2PO_4, 10 mM $NaHPO_4$, 2.5 mM KCl, pH 7.4 + 0.1% v/v Tween 20) on a bidirectional rotator to remove all remaining Ponceau S solution from the blot.

India Ink Staining

India ink was used to permanently stain the protein bands on nitrocellulose blots. The blots were immersed in 50 ml of PBST and 5 µl India ink was added to the PBST. The blot was incubated at room temperature overnight on a bidirectional rotator. The blot was then washed twice with water and allowed to air dry. A 1:10,000 dilution factor of India ink to PBST was found to yield the best results.

Antibody Probing

The nitrocellulose blot was incubated in 25 ml of 5% skim milk blocking solution (PBST + 5% w/v skim milk powder) for 1 hour at room temperature on a bidirectional rotator. After the 1 hour blocking step, 2 µl of a 1:12,500 dilution of mouse anti-V5 primary antibody (Pierce Antibodies; Rockford, IL) was added; the antibody was incubated with the blot for 1 hour at room temperature on a bidirectional rotator. Blots were also probed with each antibody specific to the added epitope tag for each gene; these antibodies were diluted 1:5000 in 4% BSA in 1x PBST. The antibody solution was removed and the blot was then washed 3 times with 25 ml of 1x PBST for 5 minutes per wash. The wash solution was replaced with 25 ml of 1x PBST, 5% w/v skim milk, 1 µl of chicken anti-mouse secondary antibody (Pierce Antibodies; Rockford, IL) conjugated with horseradish peroxidase (1:25,000 dilution) and incubated for 1 hour at room temperature on a bidirectional rotator. The secondary antibody solution was removed and the blot was washed 4 times with 25 ml 1x PBST for 5 minutes each. The PBST wash solution was replaced with 3 ml of Enhanced Chemiluminescence (ECL) reagent (1 part Luminol/enhancer, 1 part Stable Peroxide Buffer; Pierce; Rockford, IL) and mixed for 2 minutes at room temperature. The nitrocellulose membrane was removed from the ECL solution and wrapped in plastic cling wrap. The blot was exposed to X-Ray film (Kodak; Toronto, ON) in a dark room for varying amounts of time to optimize image intensity. The film was developed with an automated developer (Kodak X-OMAT 1000A, Toronto,

ON). The developed X-Ray film images were scanned on a flatbed scanner (Canon Pixma MP620; Mississauga, ON)

Antibody Stripping

To remove antibodies from a nitrocellulose blot, 150ml antibody stripping buffer (0.2M glycine, 0.5M NaCl pH 2.5 in dH_2O) was added to the blot. The blot was microwaved in the solution at 50% power in 30 second increments and shaken for 3 minutes. The antibody stripping buffer was replaced and the process was repeated x 2. The blot was then washed 3 times in PBST and blocked in PBST+5% skim milk for re-probing.

Baculovirus Protein Expression Time Course

Six 6-well adherent cell culture plates were seeded with $1.62x10^6$ cells/well in 3 ml of SF900-II media. The cells were allowed to adhere for 30 minutes prior to infection. Each baculovirus construct (CESA1, CESA3, DET3, POM1, COBRA, and ACMNV) was infected into 6 wells at a Multiplicity of Infection (MOI) of 10 pfu/cell. At the time intervals of 48, 72 and 96 hours post infection, two wells were collected for each virus; one well was processed for whole cell protein and the other was processed for membrane protein. The protein extracts were quantified using the BCA assay and electrophoresed on a 10% SDS-PAGE gel. The protein was then blotted onto nitrocellulose and probed and imaged as stated in the Western blotting protocol.

C^{14}-Glucose Incorporation

C^{14}-Glucose incorporations were carried out on 6-well adherent culture plates. Preliminary tests were carried out in triplicate, while confirmation of the preliminary

tests was carried out in sextuplet. $8x10^5$ cells were seeded per well in a 2 ml volume of SF900-II media. Cells were allowed to adhere for 30 min prior to infection. Baculoviruses were infected at an MOI of 10 pfu/cell to ensure simultaneous infection of all cells. Infections were incubated at 28^{o}C for 72 hours. At 72 hours, 1 ml of 0.5 µCi/ml C^{14}-glucose was added to each well, achieving a final concentration of 0.13 µCi/ml of C^{14}-glucose per well. The infections were incubated for a further 24 hours and harvested. Cells and media were collected from each well and transferred to 15 ml conical tube. Cells were centrifuged at 3000 x *g* and the media was decanted. 1 ml of 1M NaOH was added to each sample, and the sample was transferred to 1.5 ml screw cap tubes. Alternatively, 1 ml of Updegraff solution (10:1 80% acetic acid:nitric acid v/v) was also used to obtain only crystalline cellulose (Updegraff, 1969). The samples were heated to 95^{o}C for 1 hour. Soluble and insoluble fractions were separated using a 12 well suction filtration system (Millipore; Billerica, MA). The insoluble fractions were retained on Watman 25 mm GF/A glass microfilters. The soluble fraction was collected in 15 ml conical tubes from the flow through of microfilters. The soluble fraction was removed from the system and the insoluble portions were washed 4 x 25 ml of water and 1 x 10 ml 100% ethanol, under vacuum. The insoluble portions were allowed to dry overnight. Non-infected SF9 cells and wild type AcMNPV infected SF9 cells provide the minimum level of C^{14}-glucose incorporation. Both the insoluble fractions and the soluble fractions were transferred to scintillation vials. 5 ml of Ultima Gold high flash point scintillation liquid cocktail (Perkin Elmer; Waltham, MA) was added to each scintillation vial. C^{14}-glucose incorporation was counted using a Perkin Elmer Tri-carb 2800 liquid scintillation detector (Waltham, MA). The counts from the soluble and insoluble for each sample were expressed in counts per minute (CPM) or as percent incorporation ((insoluble/(insoluble +soluble))*100).

Results

Amplification of Target Genes

PCR amplification of each of the target genes resulted in DNA products at their expected sizes **(Table 6)**. The amplification products of *pom1* and *det3* are fainter than the others displaying lower amplification derived from either lower initial concentration of the template relative to the other genes or a lower primer binding efficiency than the other proteins. Each product was approximately 22-46 base pairs (bp) larger than its native length due to the epitope tag and the TOPO recognition tag added by the PCR primers as shown in **(Table 2).** The products were electrophoresed on a 1% agarose gel for imaging **(Figure 5)**.

Plasmid Clones

The cloned plasmids were transformed into DH5α and grown on LB agar plates containing the antibiotic Kanamycin. 10 colonies were screened for each of the transformations. The size of each plasmid was determined by cutting with the restriction enzyme NotI. NotI only cuts each of the plasmids once linearizing the plasmid, enabling the length to be determined on a 1% agarose gel **(Figure 7)**. Double restriction digests were undertaken on each construct to show directionality. The plasmids were double digested with the enzymes; *CESA1*- NotI/SmaI, *CESA3*- NotI/BamHI, *COB*- NotI/BamHI, *POM1*- NotI/KpnI, *DET3*- NotI/BglII. One plasmid from each transformation was chosen based on size and the gene inserts direction and carried forward into recombination.

Sequencing of Clones

Each of the cloned genes were sequenced in their entirety starting at the M13 forward and reverse primer sites on the pENTR/D-topo plasmid (Data not shown). These sequences aligned directly with the CDS sequences acquired from the TAIR database. There were minor alignment conflicts in the sequences flagged by the software. By visually examining the trace diagrams of the sequencing data, the conflicts

were resolved and the sequences proved to be identical to the reference sequences. The sequencing was completed by the Sanger sequencing facility at The Center for Applied Genomics at The Hospital for Sick Children.

Viral Titer Assay

For each of the baculovirus constructs a viral titer was completed to determine the number of infectious particles in each baculovirus stock. The results of the assay are shown in **(Table 6)**. Using an ACMNPV of known concentration a standard curve was developed to establish the concentration of the unknown baculovirus constructs **(Figure 8)**. The ACMNPV standard was diluted at 1:10, 1:100, 1:1000, and 1:10000. The standard curve was used to generate an equation of $y=332439e^{0.1108x}$ with an R^2 value of 0.9103.

DET3 Infected Cell Phenotype

During post-infection of the DET3 baculovirus into SF9 cells a phenotype unique to this baculovirus infected cell line was observed. The cells developed a tailing phenotype, where the cell elongates out of the cell on one side or opposite sides **(Figure 9)**. This phenotype has been observed over subsequent infections. These elongations are rarely seen in non-infected and non-DET3 baculovirus infections.

Protein Expression

The protein expression of each viral construct was analyzed through the use of western blotting techniques (Burnette, 1981). Western blots allowed for the presence or absence of the target proteins to be determined. It also allowed for a qualitative estimation of the level of protein expression and determination if the target protein was of the correct length.

The initial western blots of whole cell extracted protein were probed using antibodies to target the designed epitope tags for each protein that were added via the PCR primers **(Table 2)**. These blots that employed the designed epitope tags; C-MYC, VSV-G, HSV and FLAG resulted in no signal of the target protein (Data not shown). In one case, the probing with the V5 antibody there was cross reaction with the other target proteins. The V5 antibody was found to bind to all target proteins due to the N-terminal V5 epitope tag fused to the target gene by the baculovirus. The blot probing for DET3 via an anti-V5 antibody showed the DET3 protein in the lane for the DET3 infection and a protein consistent with CESA3 in the lane for the CESA3 baculovirus infections. CESA1 did not show any binding near the size of interest. In both CESA1 and CESA3 baculovirus infections, a band is seen at approximately 25 kDa **(Figure 10)**.

In light of the success with the anti-V5 antibody against CESA3, the remaining proteins COBRA and POM1 were also probed with the anti-V5 antibody. POM1 showed no significant signal. COBRA showed antibody binding at two locations on the blot, one at just above 66 kDa and one around 50 kDa **(Figure 11)**. Since all the target proteins were probed with the same secondary antibody, it can be concluded that each of the unique target protein bands are due to the primary antibody and not non-specific binding of the secondary antibody.

To establish the optimal time of harvesting the baculovirus infections each virus was infected into a 6 well plate, two samples for each virus were harvested at 48, 72 and 96 hours. One sample was extracted for total protein and the other sample was extracted for membrane protein. The protein expression patterns were analyzed by western blot. In the time course for CESA1, the protein showed up in very low amounts in both the 72 hour membrane fraction and the 96 hour membrane fraction. The blot was blocked with 4% BSA instead of 5% skim milk powder to increase the sensitivity of the assay. Blocking regimens suggested by the Abcam guide to Western blotting indicated that BSA would increase the signal intensity over that of skim milk powder as the blocking agent. The concentration of CESA1 protein increases as the duration of the

infection increases as can be seen in **(Figure 12).** The time course results for CESA3 show the presence of CESA3 protein in all fractions from 48 hours to 96 hours and in both total protein and membrane fractions. The amount of target protein is in higher concentration in the membrane fractions relative to the total protein fraction. The CESA3 protein concentration in both the membrane fraction and the total protein fraction is seen to increase over the time course **(Figure 13).** DET3 showed a similar pattern to the CESA3 time course. At 48 and 72 hours slightly more of the target protein was seen in the membrane fraction relative to the total protein fraction. Both fractions show very high expression of the DET3 protein. The membrane fraction at 96 hours shows substantially less protein relative to the total protein and less than the 72 hour protein fractions **(Figure 14).** The COBRA protein as in the previous blots shows two distinct bands at the two molecular weights that are expected for the two forms of the COBRA protein (Schindelman, et al., 2001). These COBRA bands are in low concentration and only visible in the membrane fractions. In the 48 hour membrane fraction for the COBRA protein there is a third band at approximately 31 kDa, this band can also be seen faintly in the ACMNPV lane, attributing this 31 kDa band to an early infection AcMNPV protein. The COBRA blot was blocked in 4% BSA rather than 5% skim milk powder to increase the sensitivity of the assay, as was done for the CESA1 blot **(Figure 15)**. All of the target proteins have unique signals not found in the ACMNPV control or between each other.

C^{14}-glucose Incorporation into Cellulose

It was necessary to determine if the synthesized proteins had cellulose synthase activity. From the protein expression time course, it was determined that 72 hours post-infection was the optimal time for protein expression for the C^{14}-glucose incorporations. To do this infected SF9 cultures were exposed to C^{14}-glucose at 72 hours post-infection and allowed to continue to incubate for 24 hours. During different trials both Updegraff (Updegraff, 1969) and 1M NaOH solutions were used to solubilize the

cellular material and leave the cellulose behind. The insoluble cellulose was then separated from the soluble fraction by vacuum filtration. Both methods have shown to have a high degree of variability in their current forms. To evaluate the amount of insoluble content of each sample, the counts per minute (CPM) of the insoluble fraction was divided by the total CPM of the insoluble and soluble fractions. (average CPM Insoluble/(average CPM Insoluble+average CPM Soluble)*100). The percentage of insoluble material per reaction was compared for each baculovirus and combinations of baculoviruses **(Figure 16, Figure 17)**. There is variation seen between the baculovirus infections based on the averages from the Updegraff solution, but the large error bars overlap. A comparison of CESA1 and DET3 in the base treatment shows no significant difference and the raw CPM counts showed very low incorporation in either fraction <200 CPM/min. A pooling of the C^{14}incorporations for the CESA1, DET3 and SF9 cell samples shows that both infected samples have an insoluble fraction increase of approximately 9% over non-infected SF9 cells **(Figure 18).**

Discussion

The study of cellulose and the cellulose synthase complexes that synthesize cellulose is key to our understanding of the plant cell wall and very important towards our ability to modify and acquire the energy locked inside cellulose. Due to the continuingly difficult task of studying cellulose synthases, it is important to establish new methods to circumvent the limitations associated with the measurement of cellulose synthase activity, the imaging of the plant plasma membrane and the determination of which proteins are required to achieve cellulose synthesis. In this study, the potential for baculoviral expression of cellulose synthase genes in *Spodoptera fruigiperda* was examined. The baculovirus system used here to express the *Arabidopsis thaliana* cellulose synthase proteins in SF9 cells was a relatively straight forward system to employ once the viral constructs had been created, but it does require a significant amount of optimization. Based on the results of the western blots the *Arabidopsis* genes of interest *CESA3* and *DET3* have been shown to be expressed at high levels in the membrane fraction. However, *CESA1* and *COBRA* are expressed in low amounts and require further viral enrichment by ganciclovir. In the cases of CESA1 and COBRA protein detection, it was necessary to block the samples with 4% BSA in PBST instead of 5% skim milk powder in PBST. This modification of the blocking allowed for an increase in the sensitivity of the antibodies but also increased the occurrence of non-specific binding of the antibodies, as can be seen in the lower portion of the blot (**Figure 14)**. Expression of *POM1* requires further investigation and troubleshooting since no protein expression was observed. It can be shown, however, that *POM1* was recombined into the baculovirus based on the amplification of a product of the expected size of *POM1* using *POM1* specific primers and amplifying off of the recombinant *POM1* baculovirus DNA **(Figure 19)**. If *POM1* was not present in the baculovirus the amplicon would have occurred at the correct size and the *POM1* specific primers would not have bound.

The protein expression based on western blotting however did not reflect the amount of protein expression that was expected based on the viral titres. The viral

titres of almost equivalent pfu/ml for each virus with the CESA1 viral stock having the highest pfu/ml out of the synthesized constructs. When infected the amount of each virus added to each infection was calculated to achieve simultaneous infection of all SF9 cells. If each of the infectious particles contained a recombinant gene then it would be expected that under equivalent infection conditions they would lead to similar protein expression as they are all controlled under the same polyhedron promoter. Since this is not the case, it can be postulated that there are non-recombinant viruses in the viral stocks that had significantly lower protein expression. This issue may be explained by the degredation of the selection agent, ganciclovir, and not selecting against non-recombinant baculoviruses. This would allow the non-recombinant virus to propagate at the same rate as the recombinant virus. If ganciclovir degradation is the issue the viral constructs can be re-enriched with new ganciclovir stocks to isolate the recombinant virus. It is also possible that there was plasmid contamination and an unknown insert was recombined into the baculovirus DNA removing the *HSV1-TK* selection gene. In this case the mechanism of selection is lost and there are two or more mixed baculoviruses competing during enrichment. The second possible cause is less likely due to the unmixed sequencing results for each plasmid stock when sequenced from upstream of the cloning region of the pENTR/D-topo plasmid into the cloned gene. If multiple plasmids had been present in the plasmid stock the DNA sequence would have resulted in a mixed template signal, where two traces are overlapped on one another. One or two steps of re-enrichment with fresh ganciclovir on each of the viral stocks would determine if the enrichment was the issue for CESA1, COBRA and POM1 viral stocks. Poor enrichment could also be determined by incubating the SF9 infections with X-gal, as there is a *lacZ* gene in the recombination site with the *HSV1-TK* gene, which would change the colour of any non-recombinant infection to blue.

The western blotting has shown that the *Arabidopsis* membrane proteins were localizing to the SF9 membranes. In comparisons between the total protein extractions and the membrane protein extractions, the target proteins were found in higher relative concentrations in the membrane fractions than the total protein fractions, showing that

they were associating with membranes. This however does not confirm that they were moving specifically to the cell membrane, where they are active in *Arabidopsis,* but instead may be associating with any cellular membrane. To determine protein localization to the cell membrane it may be possible to probe the infected SF9 cells with a fluorescein isothiocyanate (FITC) conjugated secondary antibody and image the cells using epi-fluorescent microscopy (Forzan, Wirblich, & Roy, 2004). This would allow the target proteins to be visualized within the context of the cell to determine which membranes the target proteins are localizing to.

Initially, the target proteins were to be probed with unique epitope antibodies. The epitope tags had been PCR amplified onto the 5' ends of the gene sequence. When this method was initially designed, it was not known that the N-terminal fusion would attach upstream of the designed epitope tags creating a longer extension of the protein on the N-terminal end. Because of this N-terminal fusion it appears that the antibodies that have been designed for each protein has been inhibited. The antibodies to be employed for the study are terminal epitope antibodies designed to specifically detect a terminal epitope tag. In order to function they must wrap around the end of the protein and bind to the epitope tag. Now that the designed epitope has been shifted internally within the protein by the N-terminal fusion the antibody can no longer reach around the end of the protein and bind to the epitope. This has prevented the unique epitope tags from being used. The N-terminal fusion has however provided a terminal V5 epitope which has allowed all the proteins to be probed with an anti-V5 antibody. By acquiring internal antibodies to the designed epitope tags it should still be possible to probe each protein independently.

An unexpected phenotype witnessed was the effect that DET3 had on the morphology of the SF9 cells **(Figure 9)**. The tail-like elongations seen in the DET3 infections imply that DET3 has unique activity within SF9 cells that wild-type ACMNPV and the other baculovirus constructs do not. It could be hypothesized that that DET3 is compatible or interactive with the V-ATPase components of the SF9 cells or proteins

expressed by the AcMNPV to cause this phenotype in the SF9 cells. It is also possible that DET3 is having a cytopathic effect on the in SF9 cells and the phenotype is a response to the toxicity of the DET3 protein. Exposing DET3 infected cells to V-ATPase inhibitors, such as bafilomycin, may help determine if the phenotype is indeed V-ATPase related. It may also be of interest to attempt a co-immunoprecipitation of DET3 to determine if DET3 is associating with another protein and what identity of the protein is.

The activites of the proteins in the baculovirus constructs were unable to be determined conclusively. The C^{14}-glucose incorporation assay was designed to look for the production of cellulose in the SF9 infections. The assay in its current form has proven to have a very high amount of variability as can be seen by the error bars in **(Figure 16).** As the number of sample replicates increases the variability has shown to decrease as can be seen in the box and whisker plot **(Figure 18)**. The average counts per minute (CPM) show CESA1 has a higher insoluble fraction then the other infections after the Updegraff digestion of the SF9 tissue, but due to the large error bars that overlap with the average percent CPM of the other constructs it was inconclusive. A t-test between the means of the CESA1 sample and DET3 sample of the C^{14}-glucose incorporations result in a p-value of 0.4 showing no significance between the means. After pooling several trials of CESA1 infections, DET3 infections and SF9 non-infected samples, it was evident that both infections had an increased insoluble fraction over that of the non-infected cells, but there is not a significant difference between the CESA1 and DET3 insoluble fractions. The lack of cellulose production could be due to several factors. The CESA1 proteins could be improperly folded, the protein expression could be too low to detect the cellulose production or the CESA1 could require an associated protein or molecule primer to function. The protein expression in the western blots does show that CESA1 is being expressed in very low amounts **(Figure 12)**, which would mean the amount of protein for synthesizing cellulose is very low. It is also possible that for CESA1 to begin producing cellulose a molecular primer, such as sitosterol-β-glucoside, is required to initiate synthesis (Peng, Kawagoe, Hogan, & Delmer, 2002). It has been hypothesized that the initiation of the synthesis of a glucan

chain requires more than just the UDP-glucose, but requires a glucosylated molecule that will prime the cellulose synthases. Since COBRA, DET3 and POM1 have not been indicated to have cellulose synthesis properties; this assay will not directly indicate if they are forming active proteins. COBRA, DET3 and POM1 instead are being analyzed to determine if they will modify the amount of cellulose synthase activity detected. To determine this, a clearly defined baseline of cellulose synthase activity within CESA1 alone must be established. By determining the level cellulose synthesis in CESA1 alone, the relative amount of cellulose synthesis can be compared when other proteins or substrates are added to a CESA1 infection. If the associated proteins COBRA, POM1 and DET3 are shown to have an impact on cellulose production it would be a very strong link between them and the cellulose synthases.

Conclusion

The ability to express non-native genes in the *Spodoptera frugiperda* ovarian cell is a convenient and economical system to analyze eukaryotic proteins outside of their native systems. The system incorporates very high target protein expression with glycosylation pathways similar to many eukaryotic organisms. SF9 cells also require minimal special equipment and lab certifications when compared to mammalial expression systems, which required special incubation or expression in systems such as Xenopus that require special certifications. The system is relatively straight forward to employ but does have some technical difficulties with the development of controls and check points. The preliminary application of the baculovirus system to express *Arabidopsis thaliana* membrane proteins, specifically the cellulose synthase proteins has shown promise. With the difficulties analyzing the cellulose synthase proteins of *Arabidopsis thaliana* in situ, due to the recalcitrance of the cell wall and the often embryonic lethal phenotypes of cell wall protein knockdown, the goal of the project was to express cellulose synthase proteins in SF9 insect cells via recombinant baculovirus constructs. The primary cell wall genes *CESA1* and *CESA3*, along with the cell wall associated genes *DET3, COBRA* and *POM1* were successfully amplified from cDNA and

cloned into the pENTR/D-TOPO entry vector and recombined into the *Autographa california multiple nucleocapsid polyhedron virus* genome. The recombinant proteins have been shown to be expressed during infection via Western blotting with a V5 antibody. CESA3 and DET3 are expressed in high amounts, but CESA1, COBRA and POM1 require further enrichment as their protein expression is lower than expected under the baculovirus polyhedron promoter. This has been hypothesized to be due to poor enrichment from the use of degraded ganciclovir. Comparison of total proteins samples and membrane protein samples has shown that the target proteins are localizing in the membrane fractions indicating the proteins are indeed migrating to the membranes within the SF9 cells. The DET3 baculovirus infection revealed an interesting tail-like elongation phenotype in SF9 cells. This phenotype has only been seen in the DET3 infections and requires further investigation. It may be of interest to determine how the DET3 protein is acting on the SF9 cells and if the *Arabidopsis* V-ATPase subunit is interacting with proteins from the SF9 cells or baculovirus. The C^{14}-glucose incorporation assays of the CESA proteins expressed via baculovirus infection have been inconclusive in showing cellulose synthase activity. The low CESA1 protein expression may not allow enough cellulose to be produced to be detected even if the CESA1 proteins are active. Also the C^{14}-glucose incorporation assay has a large amount of variation between replicates in its current form, making conclusive results difficult. Higher numbers of replicates have shown to reduce the error seen when analyzed. By improving the removal of the C^{14} -glucose media the variation in the replicates can be reduced. It will be important in future experiments to ensure that the proteins expressed in this experiment are localizing to the plasma membrane. Determining protein localization to the membrane could be accomplished through the use of epi-fluorescent imaging and FITC conjugated antibodies that target the V5 epitope tags. The work completed here is a baseline for future studies that could examine protein-protein interactions, purification of natively folded proteins for 3D structure analysis and analyzing stoichiometry in the event that multimeric complexes are formed.

Furthermore this work can act as a guide for those wishing to carry this research forward and aid them in the development new viral constructs.

Enzyme	Substrate	Linkage	Product	Reference
Cellulose Synthase	UDP-glucose	β -1,4-glycosidic bond	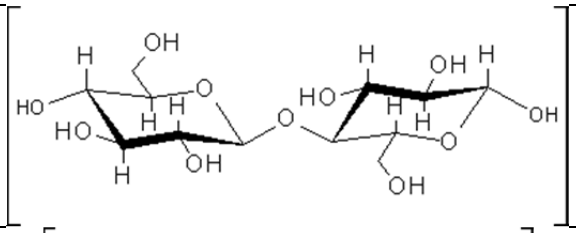	(Saxena, et al., 2001)
Hyaluronan Synthase	UDP-*N*-acetylglucosamine UDP-glucaronic acid	β -1,4-glycosidic bond β -1,3-glycosidic bond	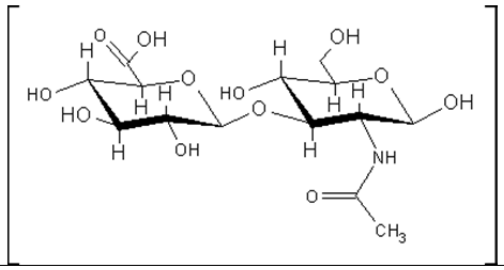	(Weigel, Hascall, & Tammi, 1997)
Chitin Synthase	UDP-*N*-acetylglucosamine	β -1,4-glycosidic bond	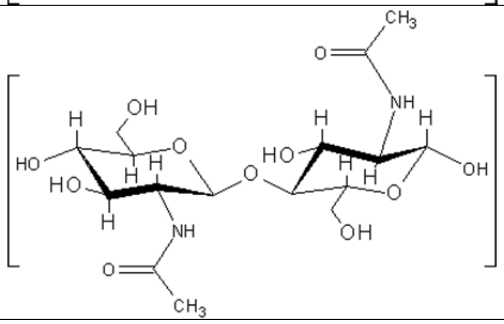	(Nagahashi et al., 1995)

Table 1. A comparison of the base units of Cellulose, Hyaluronan and Chitin. The molecular units all show a similarity in the sugar backbone of the polymers and how the structures differ in the molecular side groups.

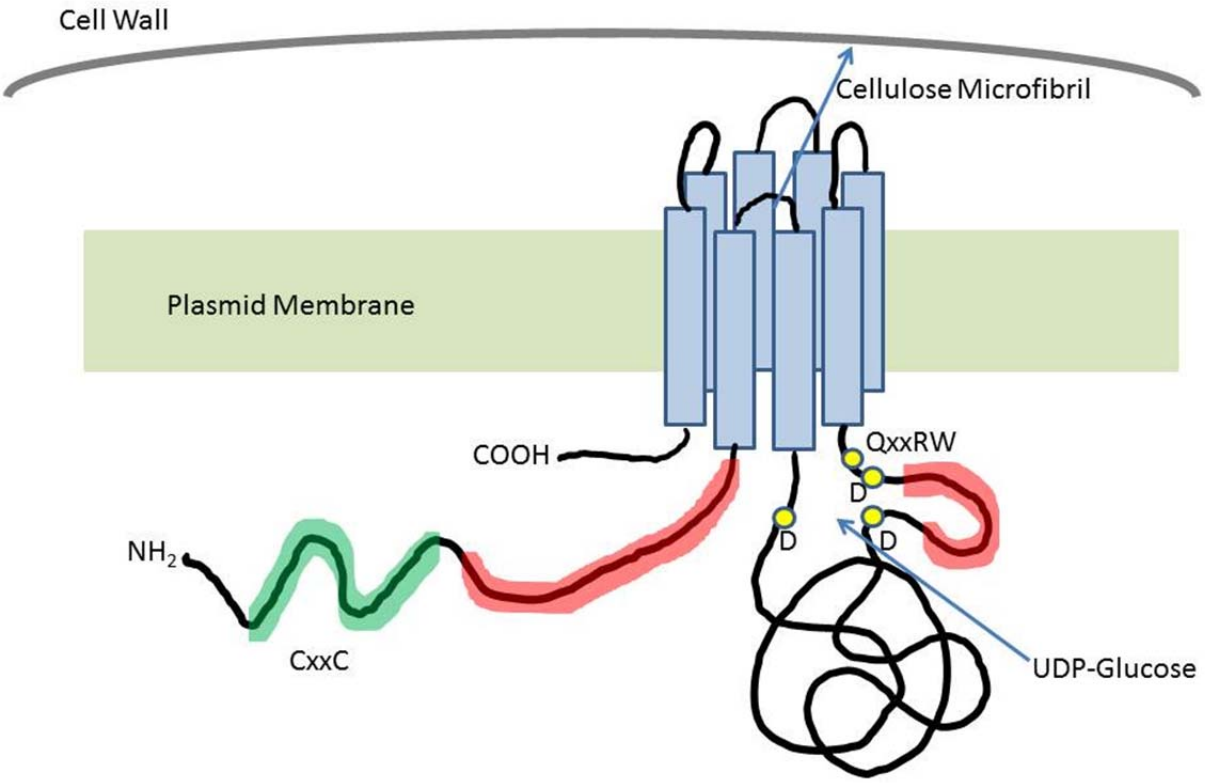

Figure 1. The hypothetical 3D-structure of a cellulose synthase protein. Image highlights the zinc finger domain (green), 8 transmembrane domains (light blue), hypervariable region (red) and the conserved regions of the catalytic domain (yellow circles). Adapted from (Richmond, 2000).

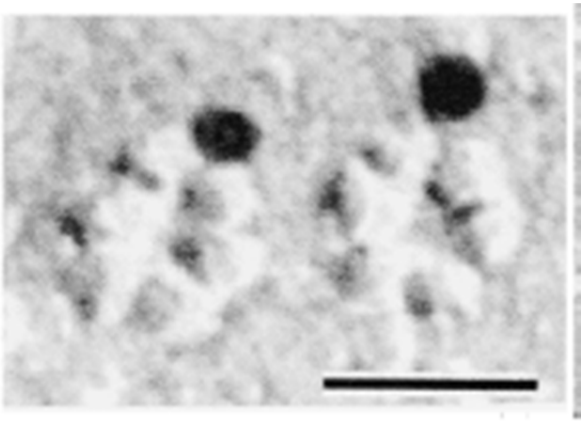

Figure 2. An electron micrograph image of a Fracture-labeled replica of a Gossypium hirsutum membrane surface showing 6 membered Rosettes. The black dot is a cellulose synthase 1 antibody bound with a gold molecule localizing to the rosettes. Bar represents 30nm. (Kimura, et al., 1999)

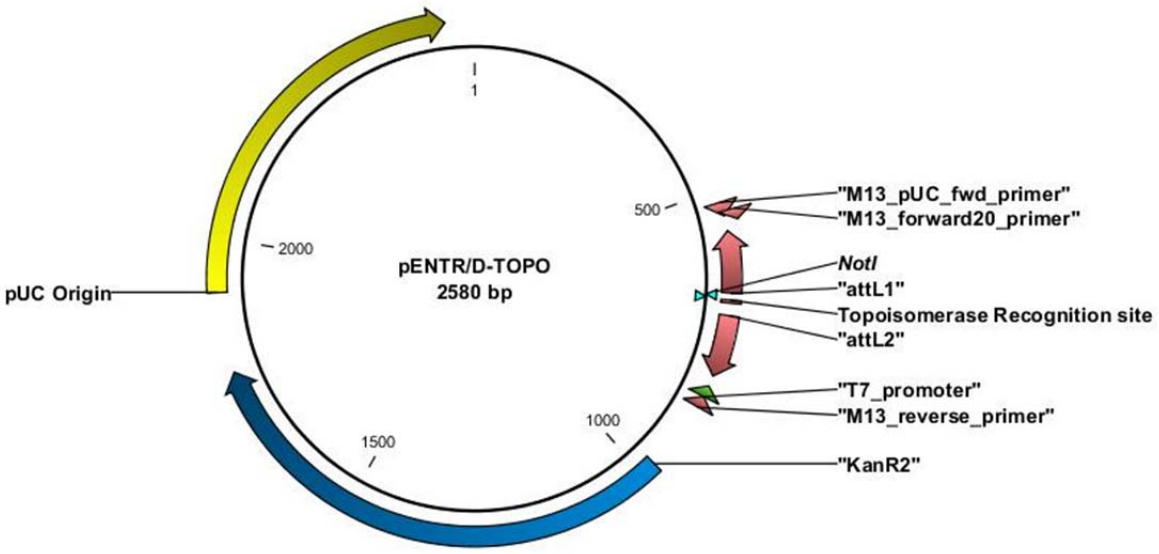

Figure 3. Plasmid map of pENTR/D-topo. The plasmid contains a kanamycin resistance gene (blue), a pUC Origin for high copy number replication in bacteria (yellow), a topoisomerase recognition site for cloning and attL1 and attL2 sites for recombination of the cloning site. There are also M13 and T7 priming sites for amplifying the cloning site**.**

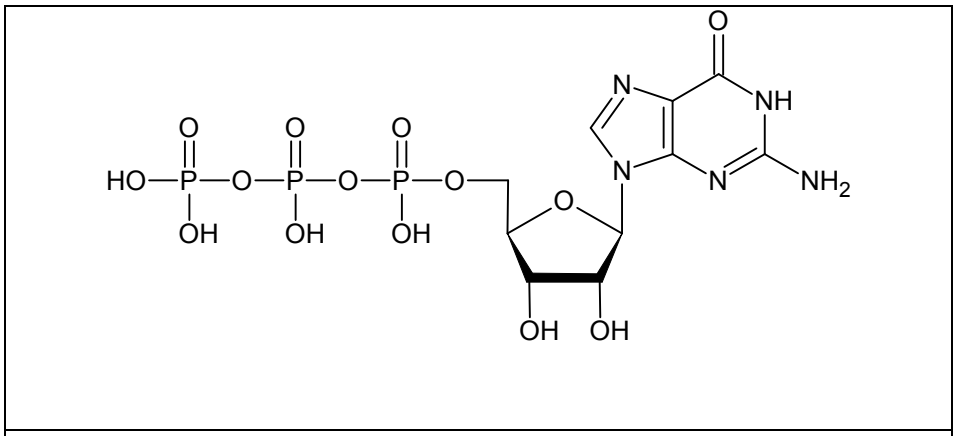

Guanosine triphosphate

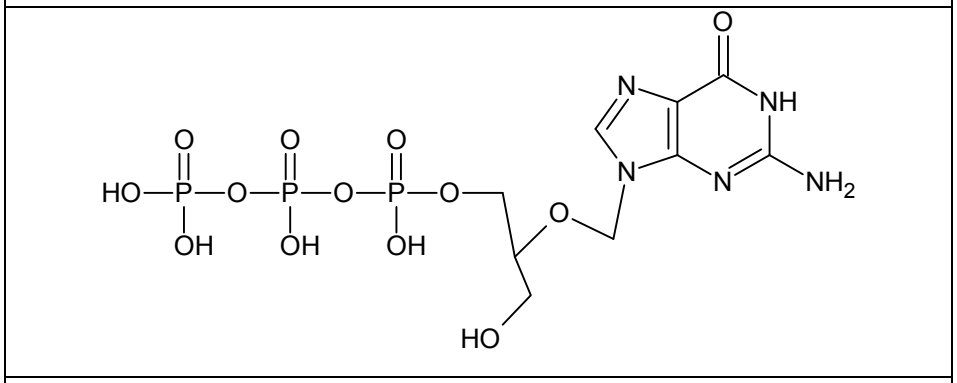

Ganciclovir triphosphate

Figure 4. Comparison of the guanosine triphosphate molecule to the ganciclovir triphosphate molecule. Where the ribose molecule is in the guanosine, the ganciclovir is lacking this ribose. This absence of the ribose prevents the next DNTP from attaching when ganciclovir is incorporated into a DNA strand and inhibits the extension of the DNA strand.

Gene	Locus	Description	Source	Epitope	Epitope Amino Acid Sequence	Epitope DNA Sequence
AtCeSA1	AT4g32410	Cell Wall Synthase Primary	cDNA	His	HHHHHH	CACCACCACCCACCACCAC
AtCeSA3	AT5g05170	Cell Wall Synthase Primary	cDNA	C-Myc	EQKLISEEDL	CACCATGGAATCCGAAGGAGAAACCG
COBRA	AT5g60920	GPI bound protein	G21905	HSV	QPELAPEDPED	CAGCCAGAGTTAGCGCCGGAGGACCCGGAGGAC
DET3	At1g12840	V-ATPase subunit C	U16695	V5	GKPIPNPLLGLDST	GGAAAGCCTATACCTAACCCTCTACTCGTACTAGACTCAACA
POM1	At1g05850	Chitinase-like protein	C00164 (E)	FLAG	DYKDDDDR	GACTACAAAGATGACGATGACCGG

Table 2. Unique epitope tags designed for each gene product. Each epitope tag corresponds to a specific antibody allowing for each protein to be probed independently.

Gene		Primer Sequence	Melting Temperature (^{o}C)	Annealing Temperature (^{o}C)
AtCeSA1	*FWD*	CACCATGCACCACCACCCACCACCACGAGGCCAGTGCCGGC	76.4	
	REV	CTAAAAGACACCTCCTTTGCCA	55.1	54
AtCeSA3	*FWD*	CACCATGGAACAAAAACTTATTTCTGAAGAAGATCTGGAATCCGAAGGAGAAACCG	66.5	
	REV	CTAACAGTTGATTCCACATTCC	51.5	54
COBRA	*FWD*	CACCATGGAGTCTTTCTTCTCCAG	57.1	
	REV	TTAGTCCTCCGGGTCCTCCGGCGCTAACTCTGGCTGGGCAGAGAAGAAGAAAA	72.6	56
DET3	*FWD*	CACCATGACTTCGAGATATTGGGTGG	59.1	
	REV	CTATGTTGAGTCTAGTACGAGTAGAGGGTTAGGTATAGGCTTTCCAGCAAGGTTGATAGTGAAGGAG	67.7	56
POM1	*FWD*	CACCATGGTGACAATCAGGAGTGGTTC	61.1	
	REV	CTACCGGTCATCGTCATCTTTGTAGTCCGAAGAGGAAGAGGAAGGTACAGTT	67.9	56

Table 3. List of gene specific primers with their melting and annealing temperatures. The primer sequences also contain the topo recognition site and the unique epitope tags.

Step	Temperature	Time
1	95^{o}C	2 minutes
2	95^{o}C	15 seconds
3	X – 1^{0}C per cycle	20 seconds
4	72^{o}C	90 seconds
5	Repeat steps 2-4 8 times, then proceed to step 6	
6	95^{o}C	15 seconds
7	X - 3^{o}C	20 seconds
8	72^{o}C	90 seconds
9	Repeat steps 6-8 30 times, then proceed to step 10	
10	72^{o}C	5 minutes
11	8^{0}C	indefinitely

Table 4. PCR conditions of a touchdown reaction. X= the melting temperature of the primer set +4 degrees Celsius.

Primer Name	Sequence 5'-3'
M13 Forward	GTAAAACGACGGCCAG
M13 Reverse	CAGGAAACAGCTATGAC
CeSA1-CDS-FWD-766bp	CTCCAAATGGCTGATGATA
CeSA1-CDS-REV-2578bp	GATAGACGATGGTGTTGA
CeSA3-CDS-REV-2513bp	TACGCAAACCTCTCAAGAA
CeSA3-CDS-FWD-540bp	GATTGTGGATCCTGTTGGA
CeSA3-CDS-FWD-462bp	CCTCTCTGTATCTTCTACT
CeSA3-CDS-FWD-1312bp	GCTATGAAGAGGGAATATG
CeSA3-CDS-FWD-2372bp	GTTCTGCTCCTATCAATC

Table 5. List of flanking and nested sequencing primers. All cloned genes were sequenced their entire lengths using flanking primers and primers nested within the genes.

Gene	Expected Gene Size (bp)
CESA1	3246
CESA3	3198
POM1	966
COBRA	1371
DET3	1128

Table 6. The expected product sizes from PCR amplification of target genes in number of base pairs. Gene lengths were determined from cDNA full length coding sequences acquired from the TAIR online database.

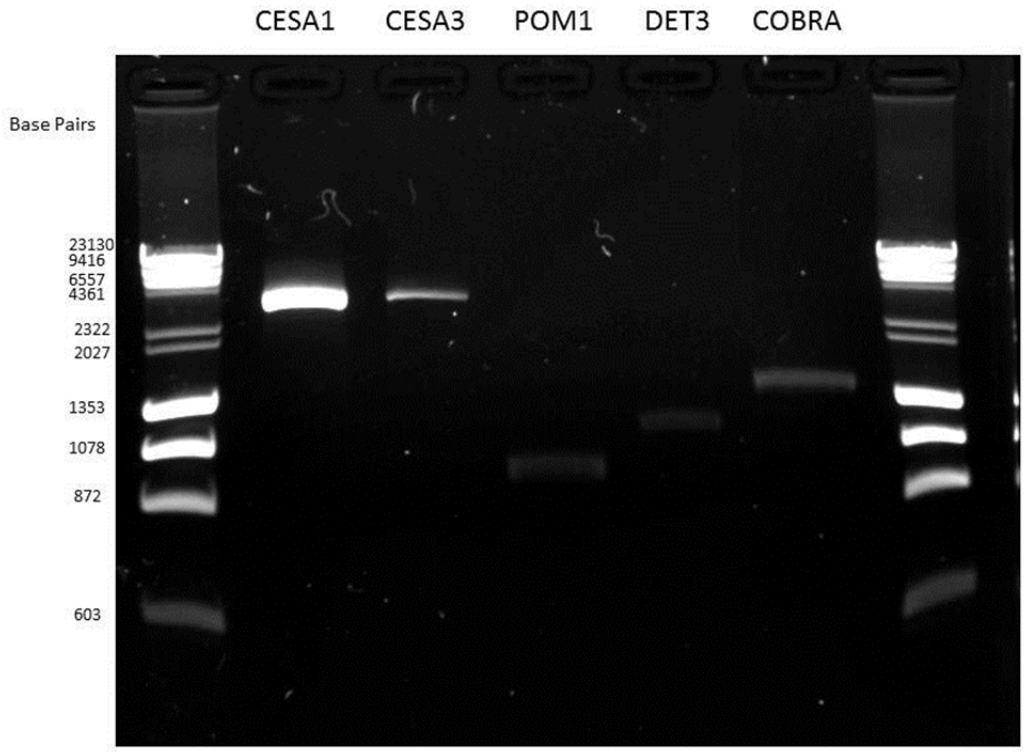

Figure 5. An agarose gel showing the PCR amplification products of CESA1, CESA3, POM1, DET3 and COBRA. The products are flanked by a broad range DNA marker #n0303 (New England Biolabs; Pickering, ON) The samples were electrophoresed on a 1% agarose gel at 100V for 35 minutes. POM1 and DET3 amplifications are very faint but present.

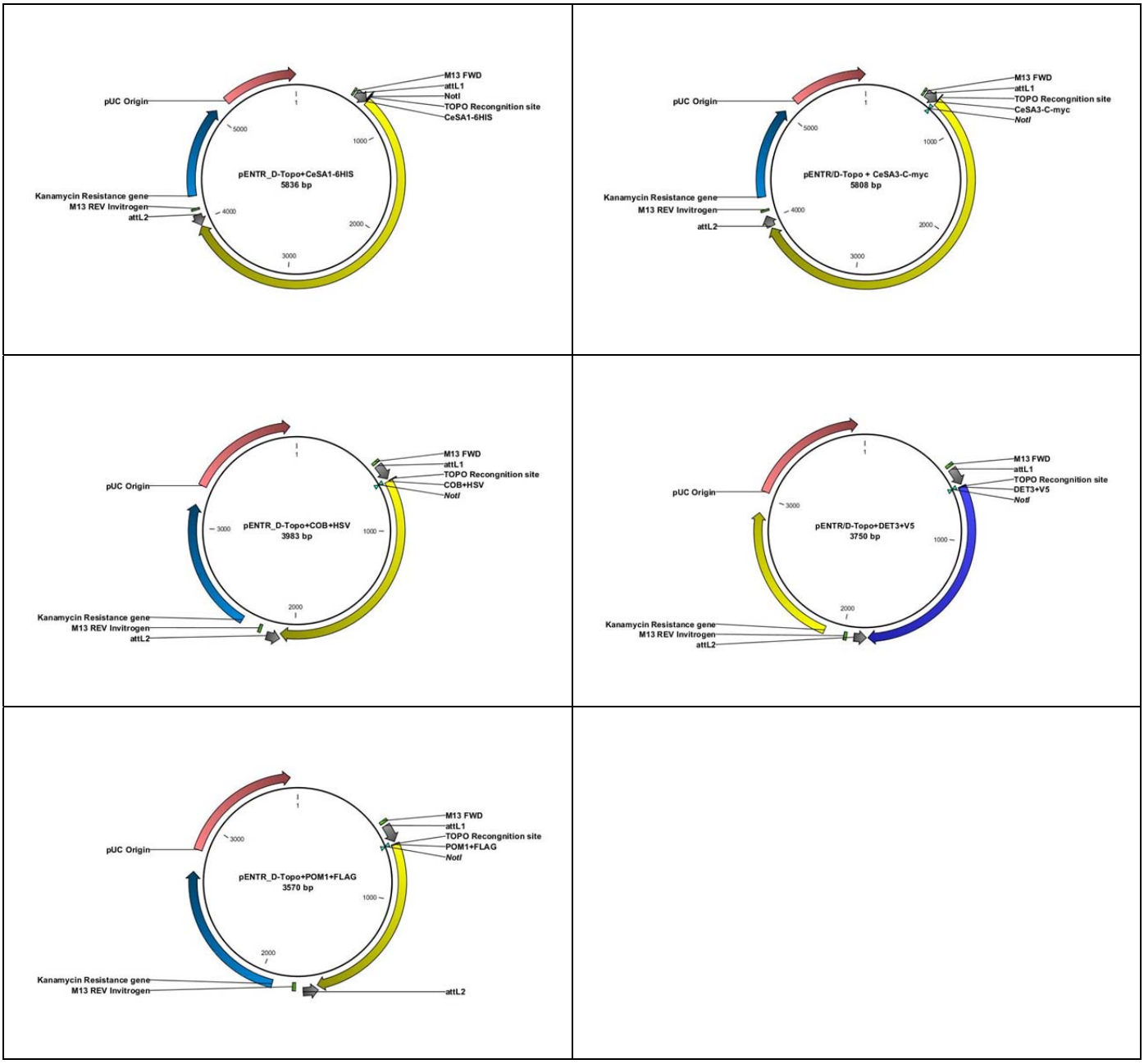

Figure 6. Plasmid Maps representing each of the pENTR/D-topo gene constructs. The plasmid maps show the location of the insert relative to the other plasmid components and the total size of each plasmid. The NotI restriction site is located directly at the 5` end of the and is a useful restriction site for plasmid analysis.

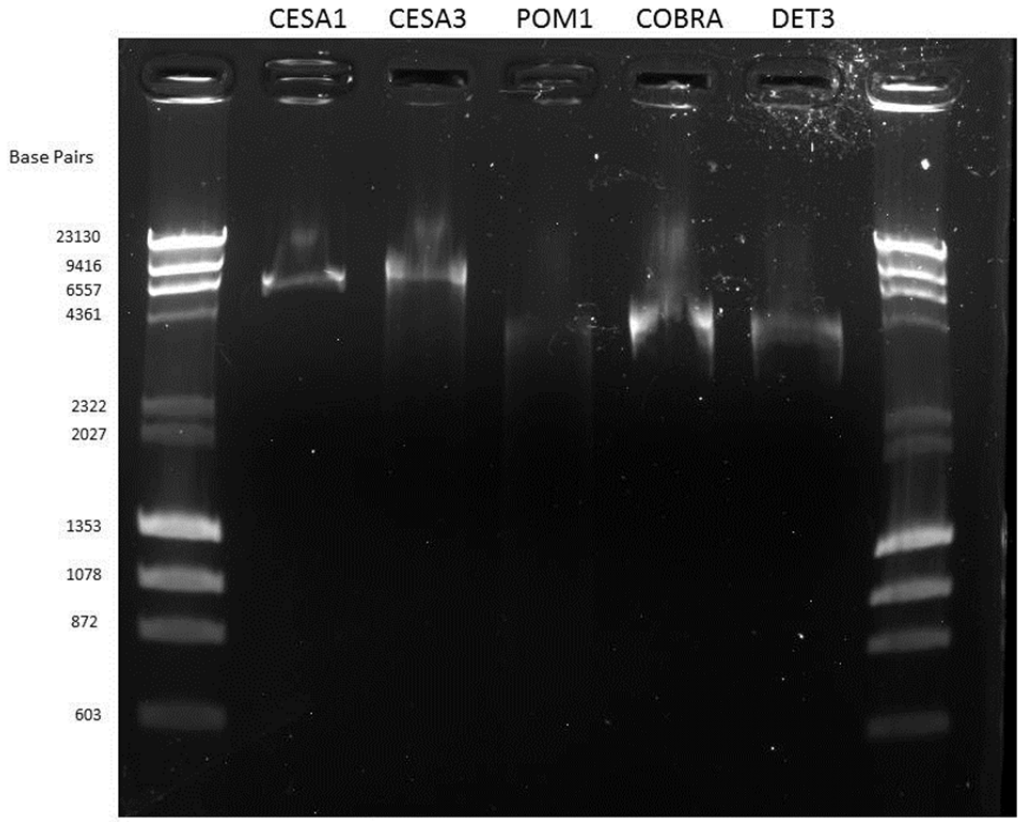

Figure 7. Plasmid constructs isolated from DH5α transformations via alkaline lysis. The plasmids were digested with the restriction enzyme NOTI for 1 hour at 37^{o}C. NOTI is a single cutting enzyme for each plasmid. The samples were electrophoresed on a 1% agarose gel at 100V for 35 minutes. The products are flanked by a broad range DNA marker #n0303 (New England Biolabs; Pickering, ON)

Virus	Titre (pfu/ml)
CeSA1	$2.56x10^8$
CeSA3	$7.63x10^7$
Det3	$1.28x10^8$
POM1	$3.62x10^7$
COB	$5.22x10^7$
ACMNPV	$3.23x10^8$

Table 7. The results of the baculovirus viral titers in pfu/ml. The titres were determined by counting SF9 cells 18 hours post-infection and comparing the ratio of non-infected to infected cells. Infected cells were determined by fluorescent detection of the gp64 surface protein expressed on infected cells.

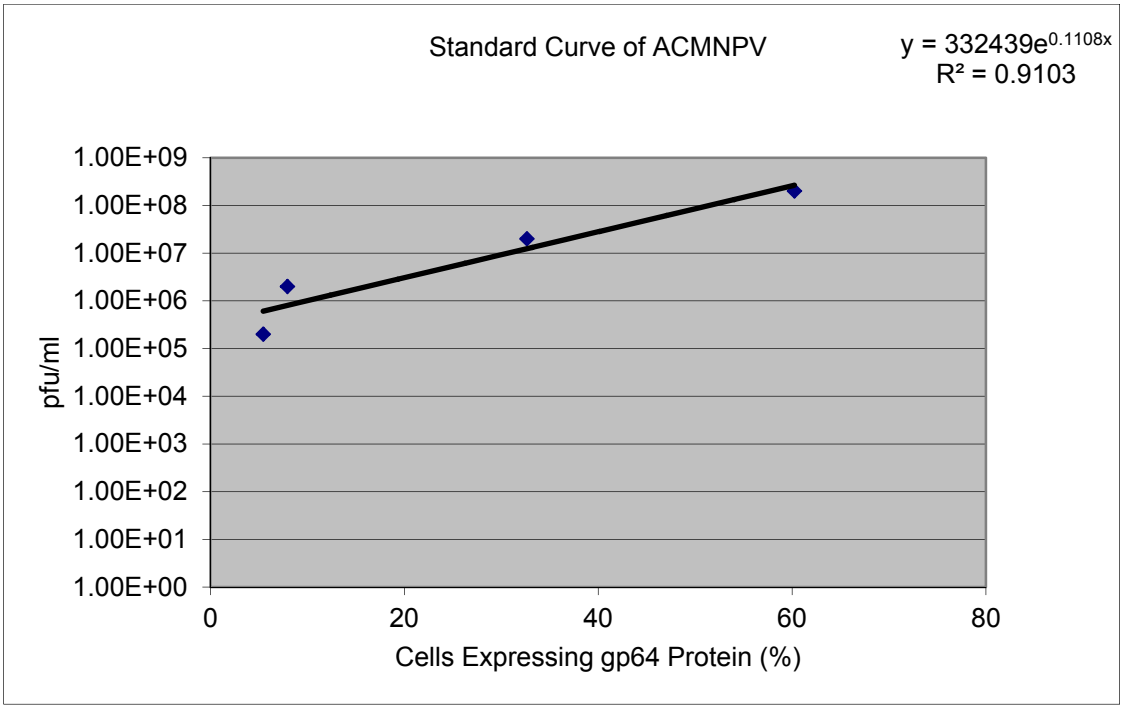

Figure 8. A standard dilution curve using AcMNPV of a known concentration of $2x10^8$ pfu/ml. Standard was diluted at 1:10, 1:100, 1:000 and 1:10000. Curve was used to establish the concentrations of the constructed baculoviruses.

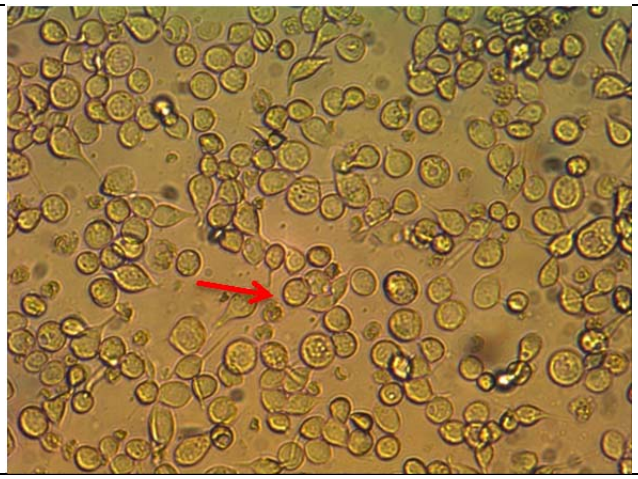

SF9 cells infected with DET3 baculovirus

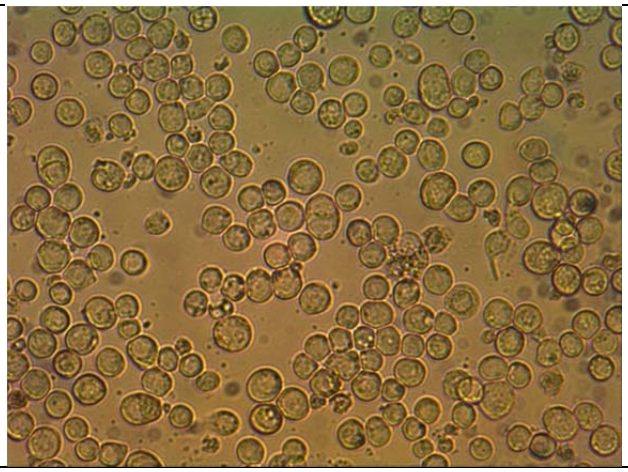

SF9 cells infected with CESA3 baculovirus

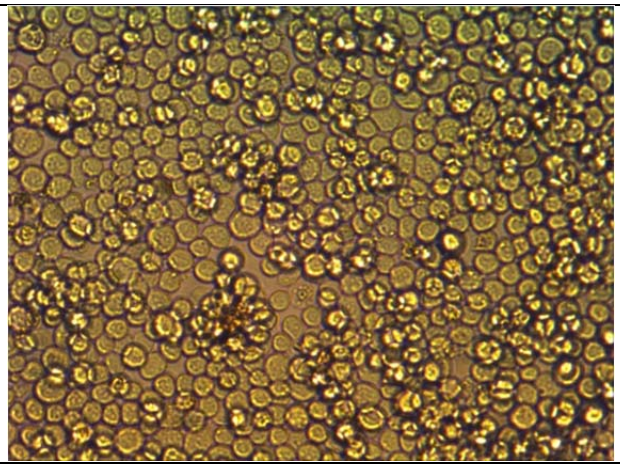

SF9 cells non-infected

Figure 9. Comparison of DET3, CESA3 and non-infected SF9 cells showing the unique DET3 phenotype. SF9 cells were seeded at $1.25X10^6$ cells per well of a 6 well plate. The reduced number of cells in the infected SF9 cells compared to the non-infected SF9 cells is due to the inhibition of cell division during infection. Images taken at 400 x magnification.

Protein	Estimated Molecular Weight (kDa)
CESA1	122
CESA3	119
POM1	35.5
COBRA	49 unmodified, 68 with GPI
DET3	42.6
HSV1-TK	25

Table 8. The estimated molecular weights of each of the target proteins (in kDa). HSV1-TK protein was also added as it may be expressed in non-recombinant baculovirus and detected during Western blots. The COBRA protein appears as two bands a 49 kDa unmodified protein and a 68 kDa protein post-translationally modified with a GPI tag.

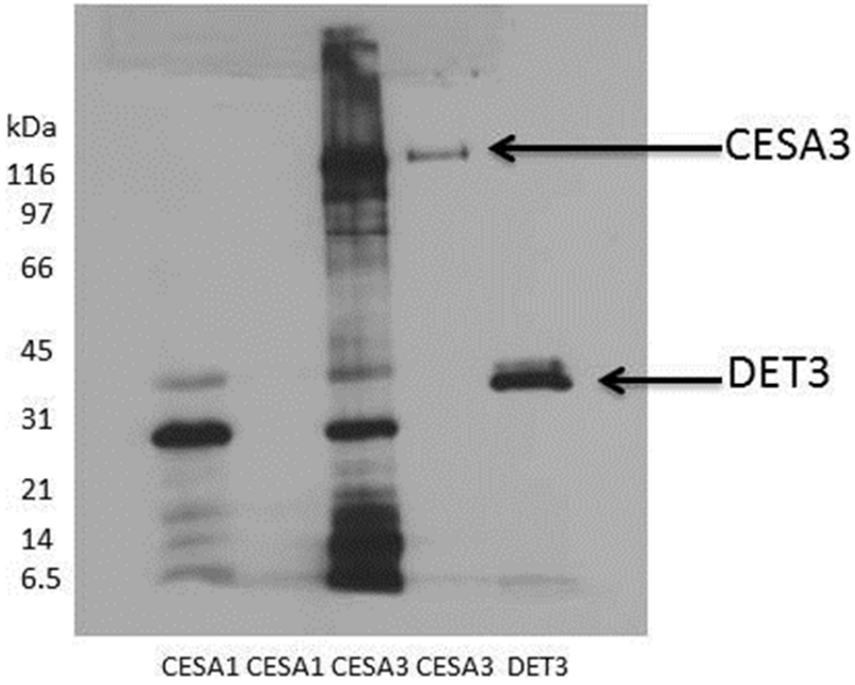

Figure 10. The anti-V5 probed western blot showing DET3 and CESA3 proteins. V5-antibody probing shows a strong signal for a protein that coincides with the estimated molecular weight of DET3. In the fourth lane the protein sample that contains the CESA3 protein shows a band at above 116 kDa. The blot was probed with mouse anti-V5 primary and chicken anti-mouse secondary. The samples were electrophoresed at 130V for approximately 1 hour in a 5%/10% SDS-PAGE stacking gel. From left to right; CESA1 40ug, CESA1 20ug, CESA3 40ug, CESA3 20ug, DET3 20ug.

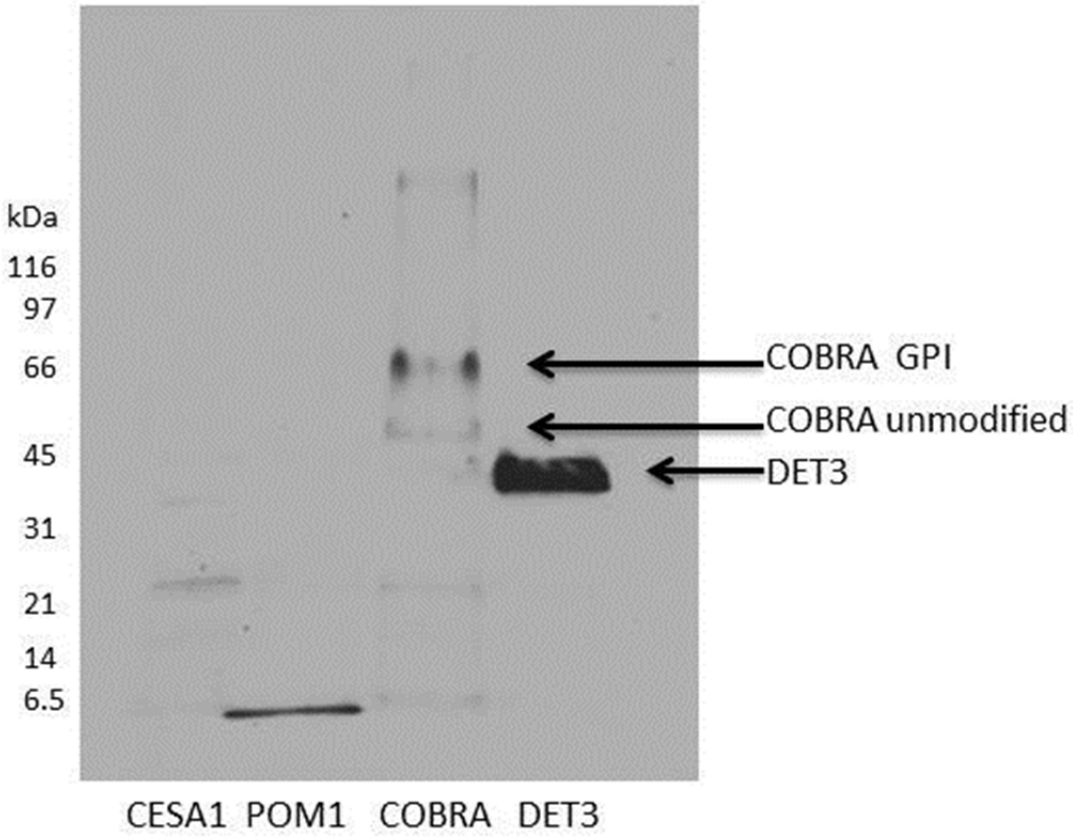

Figure 11. Anti-V5 probed western blot showing DET3 and COBRA proteins. The blot shows a dark band at 42 kDa corresponding to DET3 in lane 4. There are two bands appearing in the lane corresponding to COBRA, one just above 45 kDa and one just above 66 kDa. Both CESA1 and POM1 show no bands in the ranges that are expected for those proteins. The blot was probed with mouse anti-V5 primary and chicken anti-mouse secondary, 30 ug of total protein was loaded in each well. The samples were electrophoresed at 130V for approximately 1 hour in a 5%/10% SDS-PAGE stacking gel.

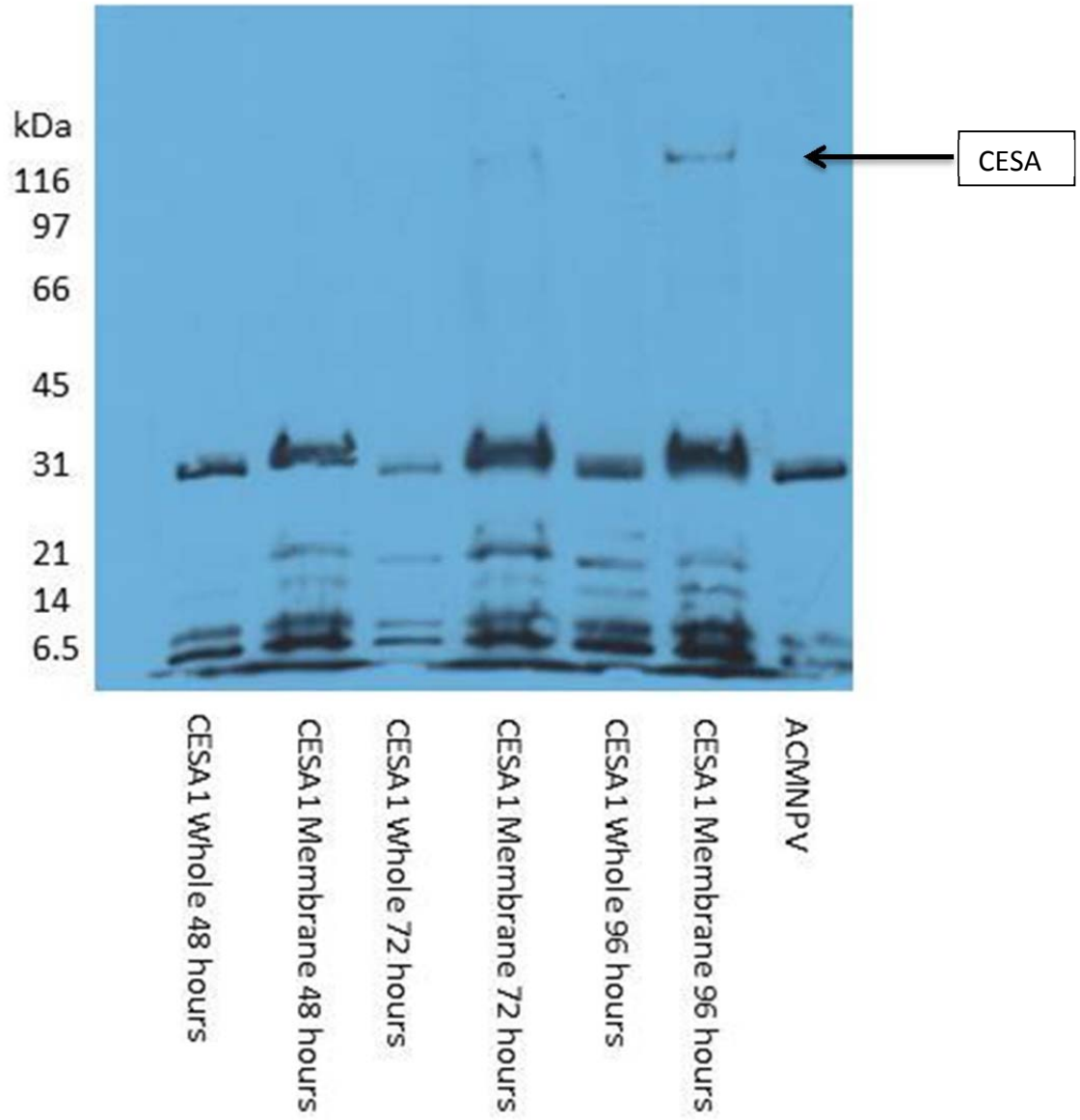

Figure 12. Time course protein extractions of both whole protein and membrane protein for the CESA1 baculovirus collected at 48, 72 and 96 hours. Faint bands are present at the molecule weight expected for CESA1. 30 ug of protein was loaded per well. The protein was electrophoresed on a 5%/10% SDS-PAGE stacking gel for approximately 1 hour at 130V. Blocked in 4% BSA in PBST.

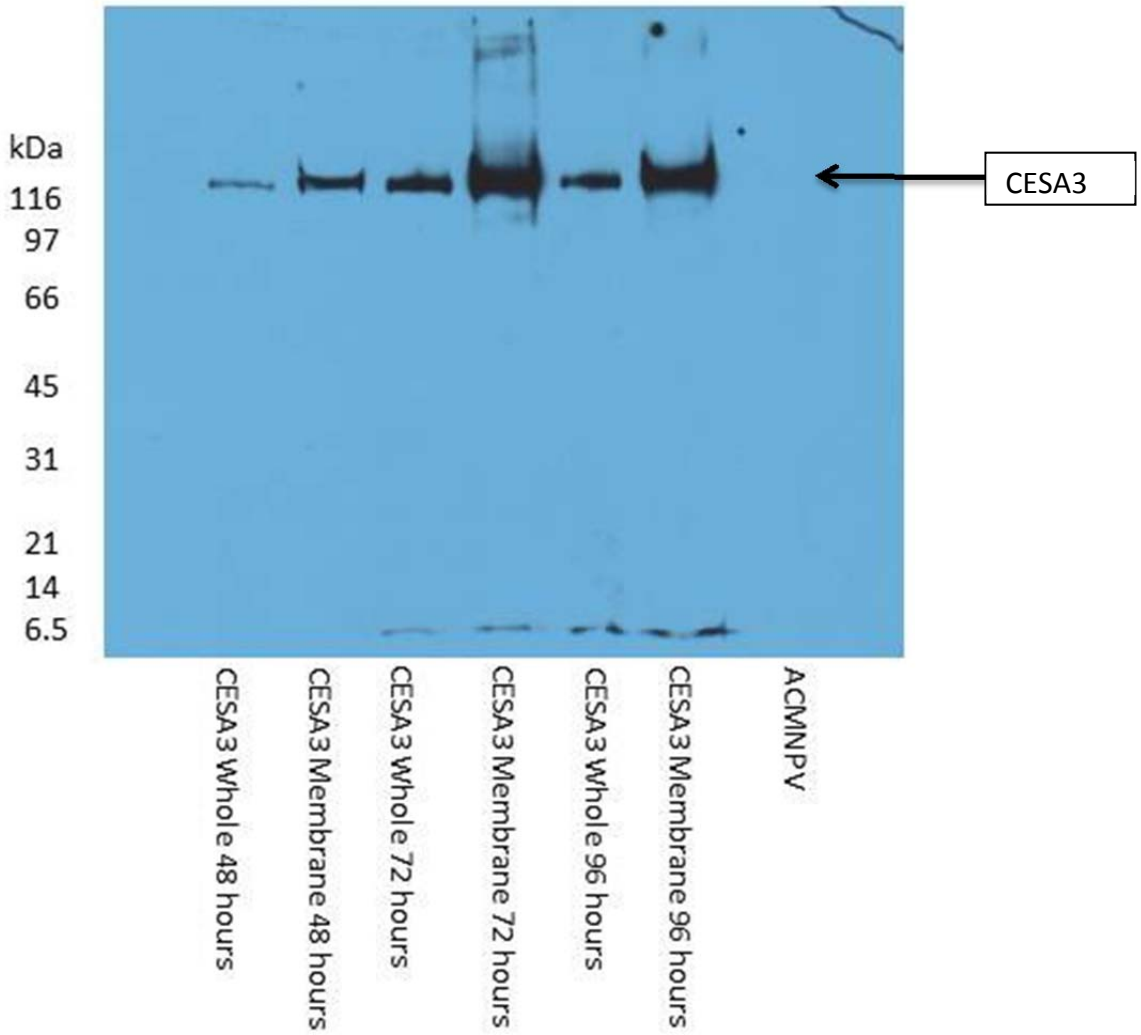

Figure 13. Time course protein extractions of both whole protein and membrane protein for the CESA3 baculovirus collected at 48, 72 and 96 hours. CESA3 bands are present at the expected molecular weight. 30 ug of protein was loaded per well. The protein was electrophoresed on a 5%/10% SDS-PAGE stacking gel for approximately 1 hour at 130V. Blot was blocked in 5% skim milk powder in PBST.

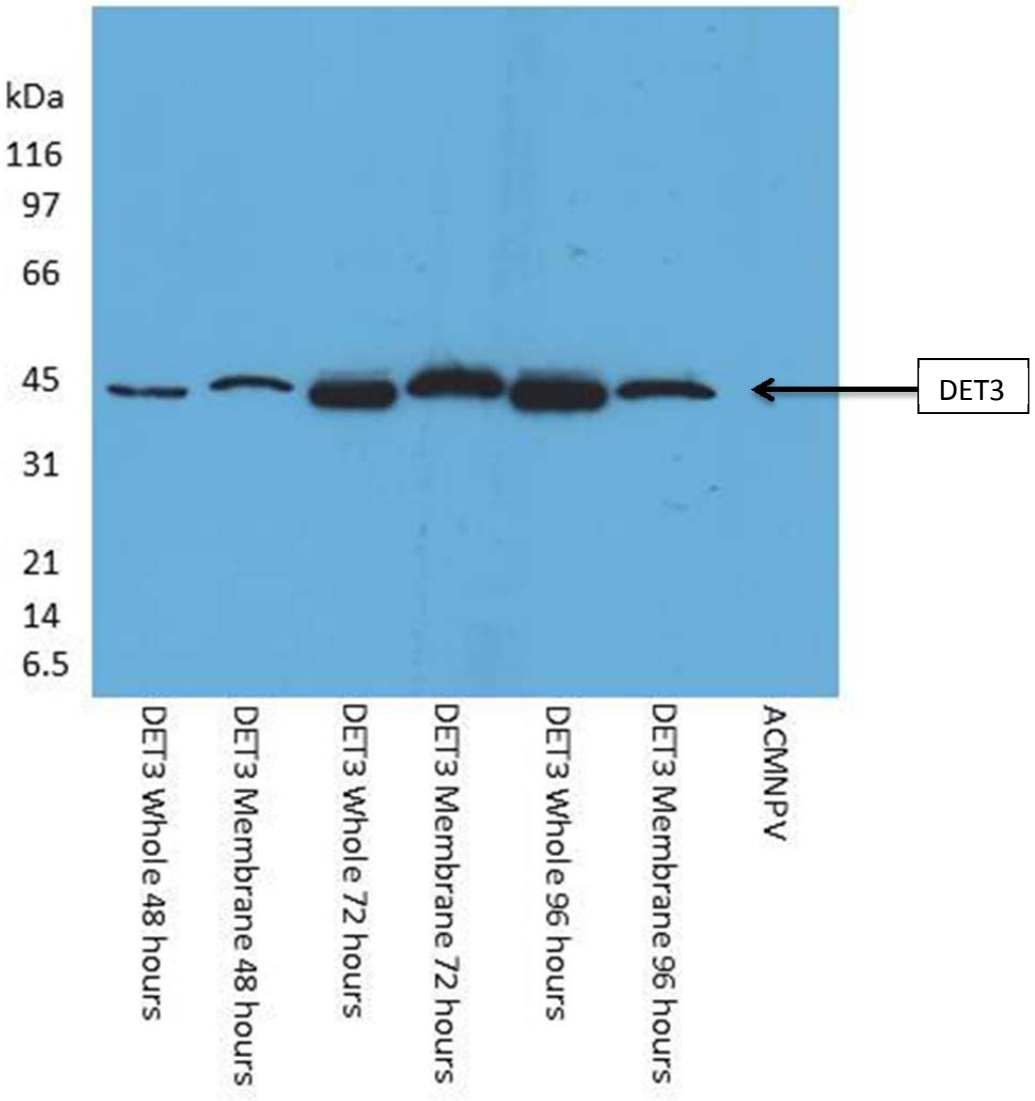

Figure 14. Time course protein extractions of both whole protein and membrane protein for the DET3 baculovirus collected at 48, 72 and 96 hours. Dark bands are present at molecule weight expected for DET3. 30 ug of protein was loaded per well. The protein was electrophoresed on a 5%/10% SDS-PAGE stacking gel for approximately 1 hour at 130V. Blot was blocked in 5% skim milk powder in PBST.

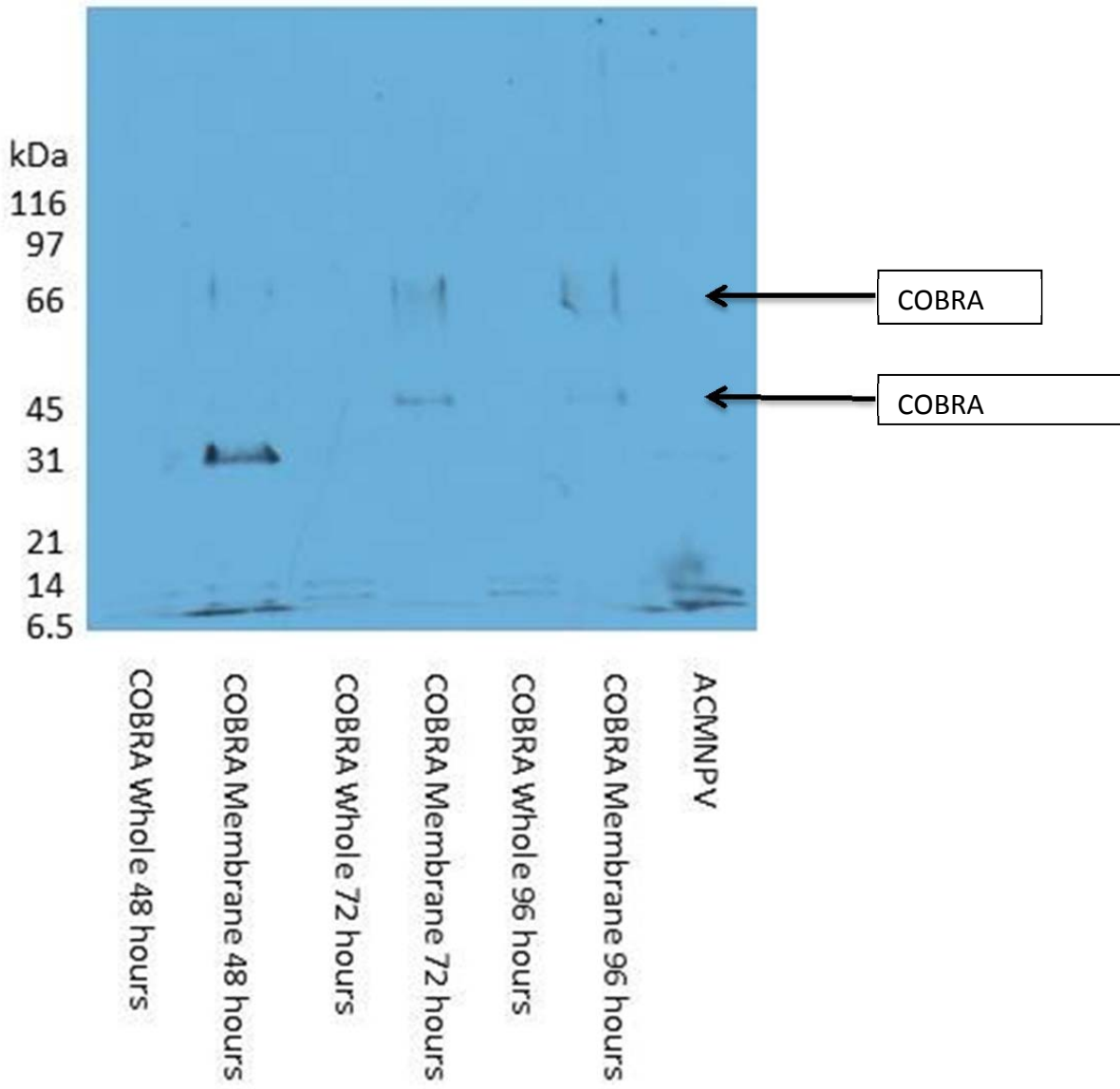

Figure 15. Time course protein extractions of both whole protein and membrane protein for the DET3 baculovirus collected at 48, 72 and 96 hours. Faint bands are present at both the molecular weights expected for COBRA. 30 ug of protein was loaded per well. The protein was electrophoresed on a 5%/10% SDS-PAGE stacking gel for approximately 1 hour at 130V. Blot was blocked in 4% BSA in PBST.

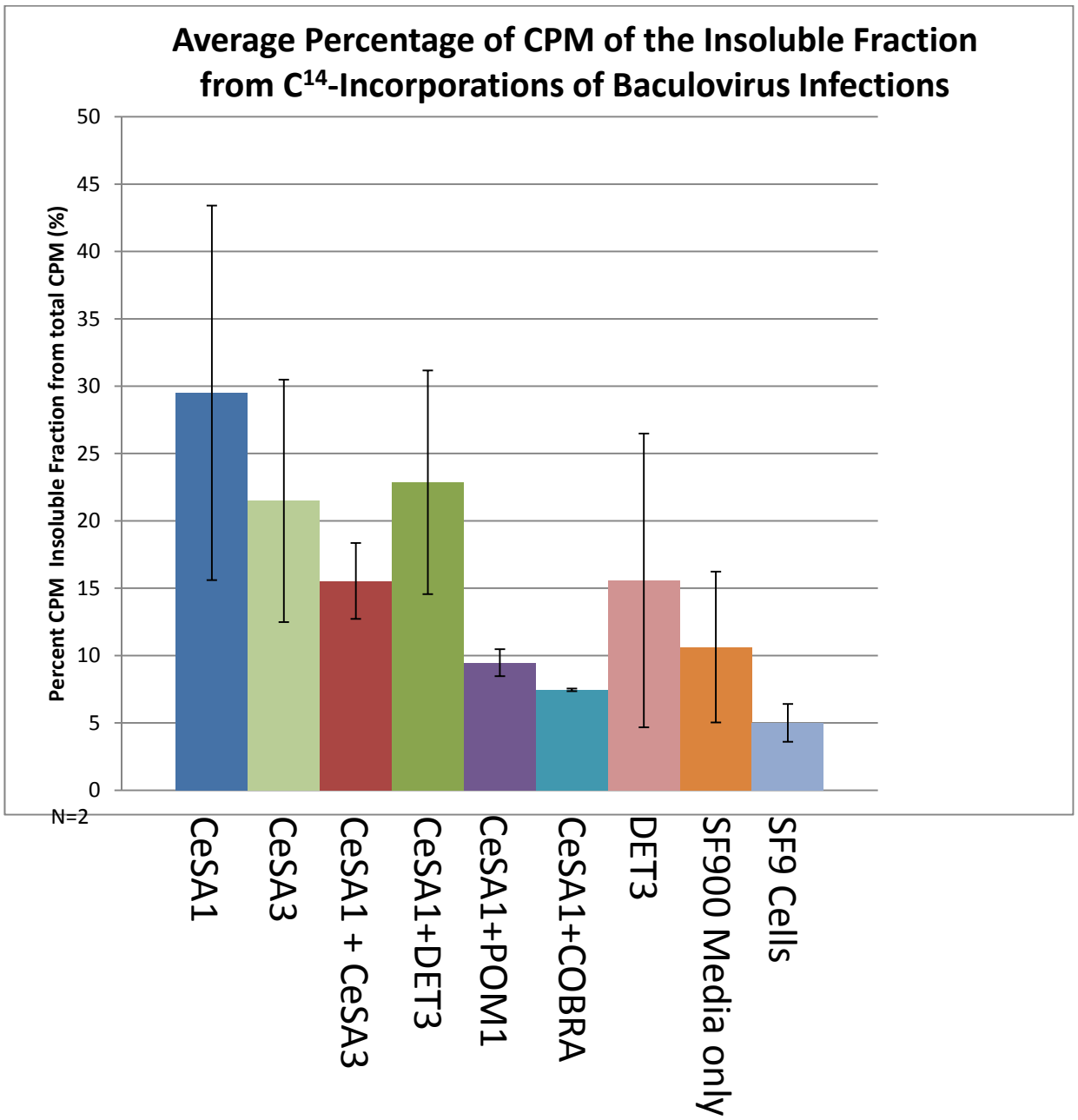

Figure 16. Graph of the Average CPM of the insoluble fractions after C14-glucose incorporation and Updegraff treatment. The graph represents the average percentage of CPM from the insoluble fraction of baculovirus infections exposed to Updegraff Solution at 100^{o}C for 1 hour. The data was derived from the equation (average CPM Insoluble/(average CPM Insoluble+average CPM Soluble)*100).

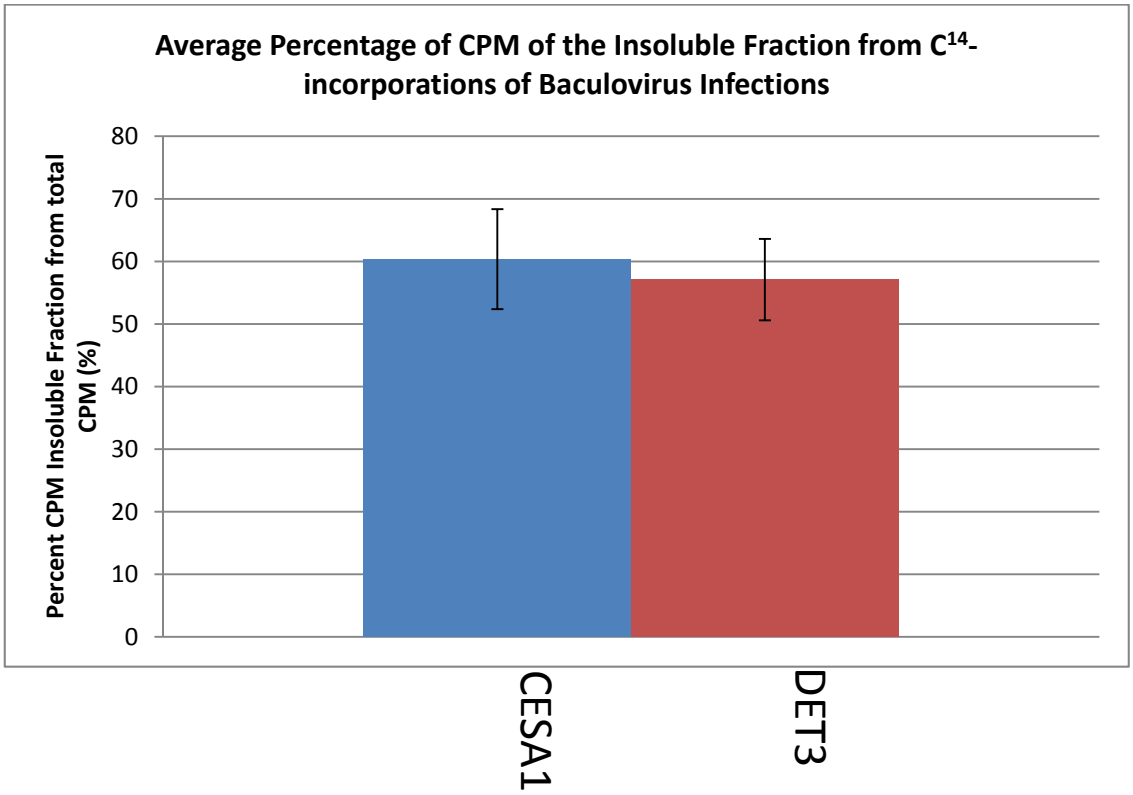

Figure 17. **Graph of the Average CPM of the insoluble fractions after C14-glucose incorporation and 1M NaOH treatment.** The graph represents the average percentage of CPM from the insoluble fraction of baculovirus infections exposed to 1M NaOH at 100^{o}C for 1 hour. The data was derived from the equation (average CPM Insoluble/(average CPM Insoluble+average CPM Soluble)*100)

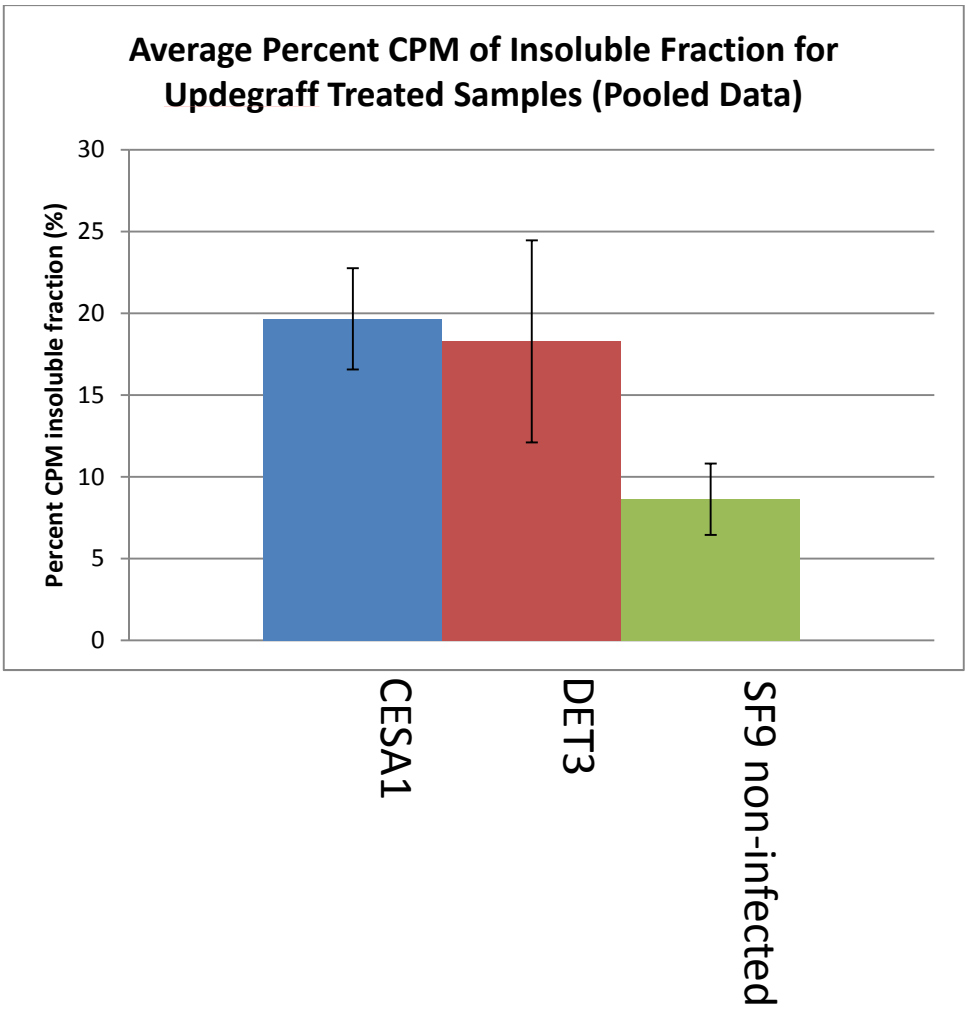

Figure 18. Graph of pooled Average CPM data for CESA1, DET3 and SF9 cells. The graph represents the pooled CPM data over several trials of C^{14}-glucose incorporation into CESA1 baculovirus infections (n=10), DET3 baculovirus infections (n=4) and non-infected SF9 cells (n=4). The average CPM counts are of the insoluble fraction after Updegraff treatment of the cell material. The percent CPM was derived using (average CPM Insoluble/(average CPM Insoluble+average CPM Soluble)*100).

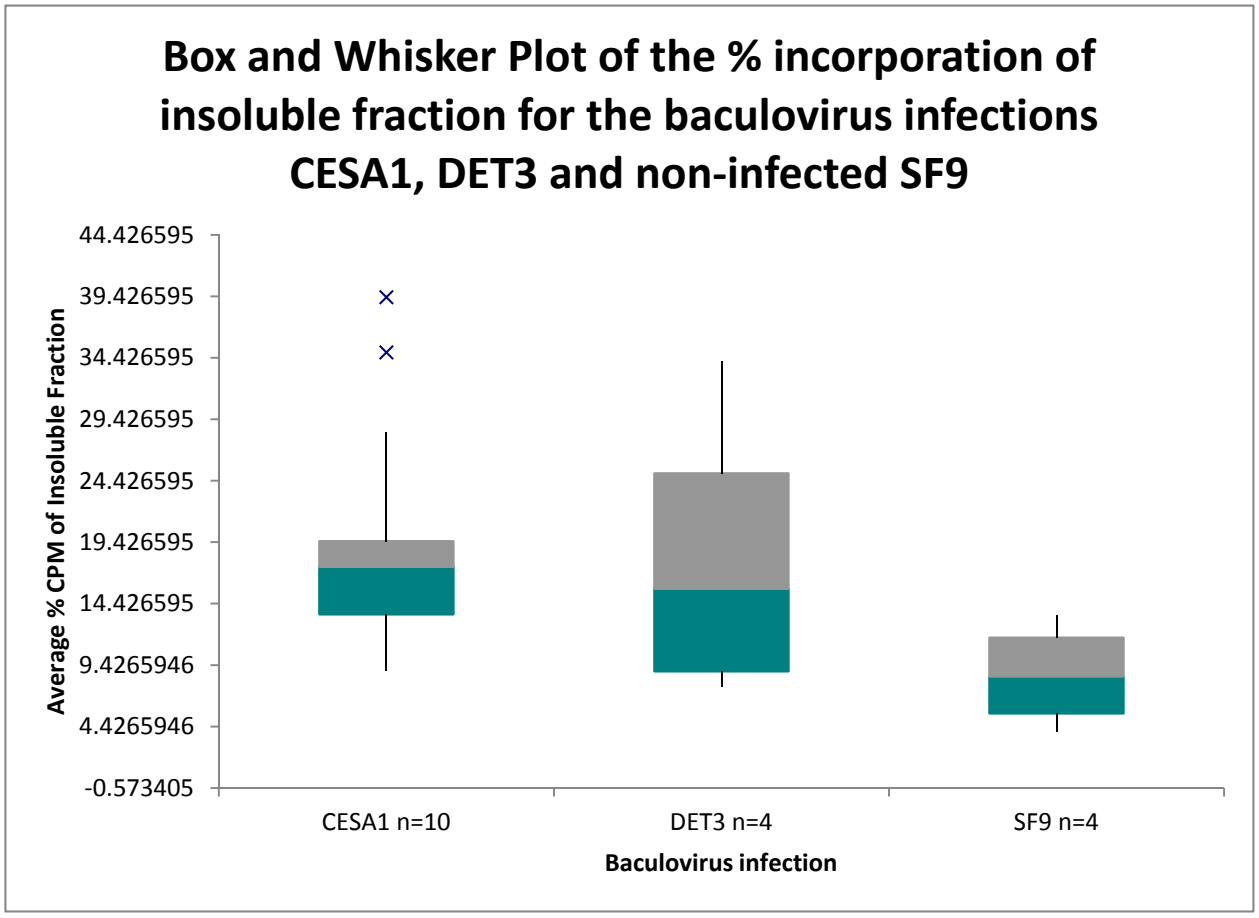

Figure 18. A box and whisker plot of the pooled replicates of CESA1, DET3 and non-infected SF9. The x marks outliers, the vertical lines mark the maximum and minimum values, the upper and lower boxes represent the upper and lower medians and the split in the box represents the median.

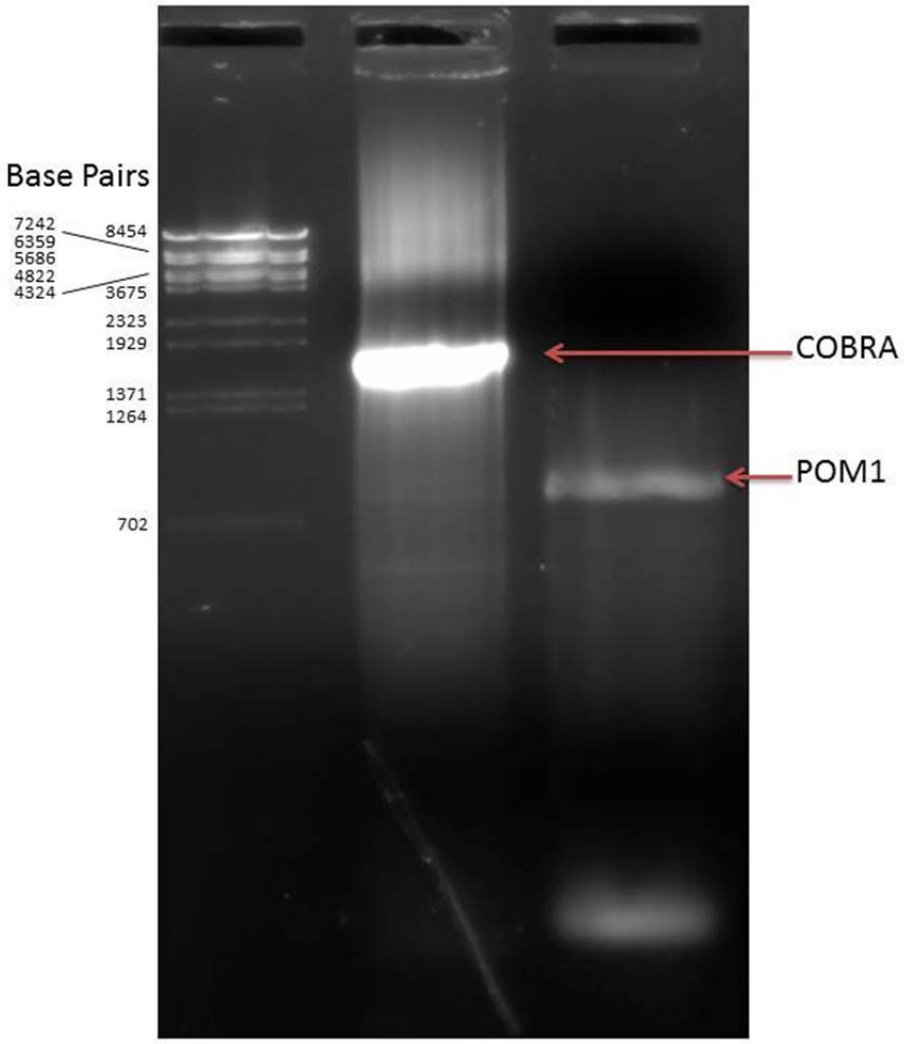

Figure 19. PCR amplification of COBRA and POM1 gene inserts from baculovirus recombinant DNA. The amplifications were primed from the Polyhedrin forward primer site in the baculovirus DNA and from the reverse primer designed specific for each gene. Based on these amplifications, it shows that the genes have been recombined into the baculovirus genome.

Permission **to Use Content from *Plant Physiology®* and *The Plant Cell***

Permission to make digital or hard copies of part or all of a work published in *Plant Physiology* or *The Plant Cell* is granted without fee for personal or classroom use, provided that copies are not made or distributed for profit or commercial advantage and that copies bear the full citation, the journal URL (www.plantphysiol.org or www.plantcell.org), and the following notice: "Copyright American Society of Plant Biologists." Please request permission in writing to reproduce material if the use is commercial or if you wish to make multiple copies other than for educational purposes. The Copyright Clearance Center is the authorized agent of ASPB for permission requests. Contact the Copyright Clearance Center at

Copyright Clearance Center Inc.
Re: *Plant Physiology®/The Plant Cell*
222 Rosewood Drive
Danvers, MA 01923 USA
Voice: 978-750-8400
Fax: 978-750-4470
Internet: http://www.copyright.com/

To Our Authors:
ASPB grants to authors whose work has been published in *Plant Physiology*® or *The Plant Cell* the royalty-free right to reuse images, portions of an article, or full articles in any book, book chapter, or journal article of which the author is the author or editor. Reproductions must bear the full citation, the journal URL (www.plantphysiol.org or www.plantcell.org), and the following notice: "Copyright American Society of Plant Biologists." ASPB further grants to authors the permission to make digital or hard copies of part or all of a work published in *Plant Physiology*® or *The Plant Cell* without fee for personal or classroom use.

References

Amor, Y., Haigler, C. H., Johnson, S., Wainscott, M., & Delmer, D. P. (1995). A membrane-associated form of sucrose synthase and its potential role in synthesis of cellulose and callose in plants. *Proc Natl Acad Sci U S A, 92*(20), 9353-9357.

Arioli, T., Peng, L., Betzner, A. S., Burn, J., Wittke, W., Herth, W., et al. (1998). Molecular analysis of cellulose biosynthesis in Arabidopsis. *Science, 279*(5351), 717-720.

Benson, D. A., Karsch-Mizrachi, I., Lipman, D. J., Ostell, J., & Wheeler, D. L. (2005). GenBank. *Nucleic Acids Res, 33*(Database issue), D34-38.

Brux, A., Liu, T. Y., Krebs, M., Stierhof, Y. D., Lohmann, J. U., Miersch, O., et al. (2008). Reduced V-ATPase activity in the trans-Golgi network causes oxylipin-dependent hypocotyl growth Inhibition in Arabidopsis. *Plant Cell, 20*(4), 1088-1100.

Burn, J. E., Hocart, C. H., Birch, R. J., Cork, A. C., & Williamson, R. E. (2002). Functional analysis of the cellulose synthase genes CesA1, CesA2, and CesA3 in Arabidopsis. *Plant Physiol, 129*(2), 797-807.

Burnette, W. N. (1981). "Western blotting": electrophoretic transfer of proteins from sodium dodecyl sulfate--polyacrylamide gels to unmodified nitrocellulose and radiographic detection with antibody and radioiodinated protein A. *Anal Biochem, 112*(2), 195-203.

Cantarel, B. L., Coutinho, P. M., Rancurel, C., Bernard, T., Lombard, V., & Henrissat, B. (2009). The Carbohydrate-Active EnZymes database (CAZy): an expert resource for Glycogenomics. *Nucleic Acids Res, 37*(Database issue), D233-238.

Cosgrove, D. J. (2005). Growth of the plant cell wall. *Nat Rev Mol Cell Biol, 6*(11), 850-861.

Coutinho, P. M., Deleury, E., Davies, G. J., & Henrissat, B. (2003). An evolving hierarchical family classification for glycosyltransferases. *J Mol Biol, 328*(2), 307-317.

Dee, K. U., & Shuler, M. L. (1997). Optimization of an assay for baculovirus titer and design of regimens for the synchronous infection of insect cells. *Biotechnol Prog, 13*(1), 14-24.

Desprez, T., Juraniec, M., Crowell, E. F., Jouy, H., Pochylova, Z., Parcy, F., et al. (2007). Organization of cellulose synthase complexes involved in primary cell wall synthesis in Arabidopsis thaliana. *Proc Natl Acad Sci U S A, 104*(39), 15572-15577.

Dettmer, J., Hong-Hermesdorf, A., Stierhof, Y. D., & Schumacher, K. (2006). Vacuolar H+-ATPase activity is required for endocytic and secretory trafficking in Arabidopsis. *Plant Cell, 18*(3), 715-730.

Farrokhi, N., Burton, R. A., Brownfield, L., Hrmova, M., Wilson, S. M., Bacic, A., et al. (2006). Plant cell wall biosynthesis: genetic, biochemical and functional genomics approaches to the identification of key genes. *Plant Biotechnol J, 4*(2), 145-167.

Forzan, M., Wirblich, C., & Roy, P. (2004). A capsid protein of nonenveloped Bluetongue virus exhibits membrane fusion activity. *Proc Natl Acad Sci U S A, 101*(7), 2100-2105.

Hauser, M. T., Morikami, A., & Benfey, P. N. (1995). Conditional root expansion mutants of Arabidopsis. *Development, 121*(4), 1237-1252.

Hermans, C., Porco, S., Verbruggen, N., & Bush, D. R. (2010). Chitinase-like protein CTL1 plays a role in altering root system architecture in response to multiple environmental conditions. *Plant Physiol, 152*(2), 904-917.

Hung, Y. H., Layton, M. J., Voskoboinik, I., Mercer, J. F., & Camakaris, J. (2007). Purification and membrane reconstitution of catalytically active Menkes copper-transporting P-type ATPase (MNK; ATP7A). *Biochem J, 401*(2), 569-579.

Kimura, S., Laosinchai, W., Itoh, T., Cui, X., Linder, C. R., & Brown, R. M., Jr. (1999). Immunogold labeling of rosette terminal cellulose-synthesizing complexes in the vascular plant vigna angularis. *Plant Cell, 11*(11), 2075-2086.

Li, S., Lei, L., Somerville, C. R., & Gu, Y. (2012). Cellulose synthase interactive protein 1 (CSI1) links microtubules and cellulose synthase complexes. *Proc Natl Acad Sci U S A, 109*(1), 185-190.

Li, X., Weng, J. K., & Chapple, C. (2008). Improvement of biomass through lignin modification. *Plant J, 54*(4), 569-581.

Liepman, A. H., Wightman, R., Geshi, N., Turner, S. R., & Scheller, H. V. (2010). Arabidopsis - a powerful model system for plant cell wall research. *Plant J, 61*(6), 1107-1121.

Nagahashi, S., Sudoh, M., Ono, N., Sawada, R., Yamaguchi, E., Uchida, Y., et al. (1995). Characterization of chitin synthase 2 of Saccharomyces cerevisiae. Implication of two highly conserved domains as possible catalytic sites. *J Biol Chem, 270*(23), 13961-13967.

Paredez, A. R., Somerville, C. R., & Ehrhardt, D. W. (2006). Visualization of cellulose synthase demonstrates functional association with microtubules. *Science, 312*(5779), 1491-1495.

Peng, L., Kawagoe, Y., Hogan, P., & Delmer, D. (2002). Sitosterol-beta-glucoside as primer for cellulose synthesis in plants. *Science, 295*(5552), 147-150.

Persson, S., Paredez, A., Carroll, A., Palsdottir, H., Doblin, M., Poindexter, P., et al. (2007). Genetic evidence for three unique components in primary cell-wall cellulose synthase complexes in Arabidopsis. *Proc Natl Acad Sci U S A, 104*(39), 15566-15571.

Richmond, T. (2000). Higher plant cellulose synthases. *Genome Biol, 1*(4), REVIEWS3001.

Roudier, F., Fernandez, A. G., Fujita, M., Himmelspach, R., Borner, G. H., Schindelman, G., et al. (2005). COBRA, an Arabidopsis extracellular glycosyl-phosphatidyl inositol-anchored protein, specifically controls highly anisotropic expansion through its involvement in cellulose microfibril orientation. *Plant Cell, 17*(6), 1749-1763.

Sambrook, J., & Russell, D. W. (Eds.). (2001). *Molecular Cloning: A Laboratory Manual, Third Edition* (Third Edition ed.). Cold Spring Harbour: Cold Spring Harbour Laboratory Press

Sanchez-Rodriguez, C., Bauer, S., Hematy, K., Saxe, F., Ibanez, A. B., Vodermaier, V., et al. (2012). Chitinase-like1/pom-pom1 and its homolog CTL2 are glucan-interacting proteins important for cellulose biosynthesis in Arabidopsis. *Plant Cell, 24*(2), 589-607.

Saxena, I. M., Brown, R. M., Jr., & Dandekar, T. (2001). Structure--function characterization of cellulose synthase: relationship to other glycosyltransferases. *Phytochemistry, 57*(7), 1135-1148.

Schindelman, G., Morikami, A., Jung, J., Baskin, T. I., Carpita, N. C., Derbyshire, P., et al. (2001). COBRA encodes a putative GPI-anchored protein, which is polarly localized and necessary for oriented cell expansion in Arabidopsis. *Genes Dev, 15*(9), 1115-1127.

Schumacher, K., Vafeados, D., McCarthy, M., Sze, H., Wilkins, T., & Chory, J. (1999). The Arabidopsis det3 mutant reveals a central role for the vacuolar H(+)-ATPase in plant growth and development. *Genes Dev, 13*(24), 3259-3270.

Simon, I., Glasser, L., & Scheraga, H. (1988). Structure of Cellulose. 2. Low-Energy Crystalline Arrangements. *Macromolecules, 21*, 8.

Somerville, C. (2006). Cellulose synthesis in higher plants. *Annu Rev Cell Dev Biol, 22*, 53-78.

Sticklen, M. (2006). Plant genetic engineering to improve biomass characteristics for biofuels. *Curr Opin Biotechnol, 17*(3), 315-319.

Sugimoto, K., Himmelspach, R., Williamson, R. E., & Wasteneys, G. O. (2003). Mutation or drug-dependent microtubule disruption causes radial swelling without altering parallel cellulose microfibril deposition in Arabidopsis root cells. *Plant Cell, 15*(6), 1414-1429.

Updegraff, D. M. (1969). Semimicro determination of cellulose in biological materials. *Anal Biochem, 32*(3), 420-424.

Weigel, P. H., Hascall, V. C., & Tammi, M. (1997). Hyaluronan synthases. *J Biol Chem, 272*(22), 13997-14000.

Whittington, A. T., Vugrek, O., Wei, K. J., Hasenbein, N. G., Sugimoto, K., Rashbrooke, M. C., et al. (2001). MOR1 is essential for organizing cortical microtubules in plants. *Nature, 411*(6837), 610-613.

Yamada, K., Lim, J., Dale, J. M., Chen, H., Shinn, P., Palm, C. J., et al. (2003). Empirical analysis of transcriptional activity in the Arabidopsis genome. *Science, 302*(5646), 842-846.